AKADEMIA GÓRNICZO-HUTNICZA IM. STANISŁAWA STASZICA W KRAKOWIE

WYDZIAŁ INFORMATYKI, ELEKTRONIKI I TELEKOMUNIKACJI

KATEDRA INFORMATYKI

PRACA DYPLOMOWA MAGISTERSKA

Quantum walks in image segmentation

Zastosowanie błądzenia kwantowego do segmentacji obrazów

Autor: ***Michał Krok***
Kierunek studiów: Informatyka
Opiekun pracy: *dr inż. Katarzyna Rycerz*
Konsultacja merytoryczna: *dr hab. inż. Piotr Gawron, IITiS PAN*

Kraków, 2018

Uprzedzony o odpowiedzialności karnej na podstawie art. 115 ust. 1 i 2 ustawy z dnia 4 lutego 1994 r. o prawie autorskim i prawach pokrewnych (t.j. Dz.U. z 2006 r. Nr 90, poz. 631 z późn. zm.): „ Kto przywłaszcza sobie autorstwo albo wprowadza w błąd co do autorstwa całości lub części cudzego utworu albo artystycznego wykonania, podlega grzywnie, karze ograniczenia wolności albo pozbawienia wolności do lat 3. Tej samej karze podlega, kto rozpowszechnia bez podania nazwiska lub pseudonimu twórcy cudzy utwór w wersji oryginalnej albo w postaci opracowania, artystyczne wykonanie albo publicznie zniekształca taki utwór, artystyczne wykonanie, fonogram, wideogram lub nadanie.”, a także uprzedzony o odpowiedzialności dyscyplinarnej na podstawie art. 211 ust. 1 ustawy z dnia 27 lipca 2005 r. Prawo o szkolnictwie wyższym (t.j. Dz. U. z 2012 r. poz. 572, z późn. zm.) „Za naruszenie przepisów obowiązujących w uczelni oraz za czyny uchybiające godności studenta student ponosi odpowiedzialność dyscyplinarną przed komisją dyscyplinarną albo przed sądem koleżeńskim samorządu studenckiego, zwanym dalej „sądem koleżeńskim”, oświadczam, że niniejszą pracę dyplomową wykonałem(-am) osobiście i samodzielnie i że nie korzystałem(-am) ze źródeł innych niż wymienione w pracy.

Abstract

Taking into consideration recent rapid developments in field of quantum information technology and more and more brave attempts to finally construct a fully functional quantum computer (like for example IBM-Q or Rigetti), it is reasonable to seek for quantum solutions that would not only answer some theoretical problems, but also could be applied to ordinary, everyday tasks. This work takes up a challenge of developing an algorithm for performing image segmentation with utilization of quantum walks, a very promising quantum computational model that is a derivative of a hugely successful classical computational framework, namely random walks. Grady [1] has provided a clever solution for image segmentation based on the random walks. Taking inspiration from Grady's work, this thesis proposes three methods of image segmentation: two algorithms harnessing quantum walks and one, which is quantum walk inspired, but is not a full-fledged quantum solution. All three methods have been simulated on a classical computer and provided results of comparable accuracy to the reference Grady's method.

Streszczenie

Biorąc pod uwagę gwałtowny postęp w dziedzinie technologii kwantowej oraz coraz śmielsze próby skonstruowania w pełni funkcjonalnego komputera kwantowego (jak na przykład IBM-Q lub Rigetti), uzasadnionym jest poszukiwanie kwantowych rozwiązań, które nie tylko rozwiązywałyby pewne teoretyczne problemy, ale także pozwoliły na wykonywanie codziennych, praktycznych zadań. Niniejsza praca podejmuje wyzwanie opracowania algorytmu służącego do segmentacji obrazu z wykorzystaniem błądzenia kwantowego. Jest to obiecujący model obliczeń, który powstał na bazie błądzenia klasycznego stosowanego z powodzeniem do wielu rozwiązań. Grady [1] zaproponował ciekawy algorytm segmentacji obrazu oparty właśnie na błądzeniu klasycznym. Czerpiąc inspirację z jego rozwiązania, niniejsza praca przedstawia trzy metody segmentacji obrazu: dwa algorytmy wykorzystujące błądzenie kwantowe oraz jeden algorytm inspirowany kwantowo, który jednak nie jest pełnoprawnym rozwiązaniem kwantowym. Wszystkie trzy rozwiązania zostały przetestowane z wykorzystaniem symulacji na komputerze klasycznym, a otrzymane rezultaty są zadowalające i wykazują na jakość segmentacji porównywalną z wynikami metody Grady'ego.

Acknowledgements

I would like to thank my supervisor, Dr. inż. Katarzyna Rycerz, for her patience, constant motivation to work, taking care of all organizational matters and creating a friendly atmosphere favorable for development and knowledge exchange between students.

I am also thanking Dr. hab. inż. Piotr Gawron from Institute of Theoretical and Applied Informatics of Polish Academy of Sciences, for sharing his vast knowledge in the field of quantum computing, sketching the directions of the work, exchanging ideas, and any tips that allowed me to finish my master's thesis.

I would also like to mention the invaluable support of my friends, Patryk Skalski and Wojciech Zagrajczuk, who were always ready to offer help and a good word and with whom we have often conducted fruitful discussions that helped me to advance in my research work.

My most heartfelt thanks go to my mother, who constantly supported me, shared her experience and good advice, repeatedly review this text and appreciated the effort put into this master's thesis.

I must also mention that the research was partially financed by the National Science Centre, Poland—project number 2014/15/B/ST6/05204.

Contents

Chapter 1

Introduction

This chapter introduces the reader with the main area of research of this thesis, namely quantum computation and quantum walks, in the section 1.1. Then, in sections 1.2 and 1.3, there are presented motivation and goal of this work, respectively. It is followed by a discussion concerning hitherto research in the fields overlapping with the thesis, in section 1.4. Finally, there is described scope and structure of this document, in section 1.5.

1.1 Quantum computation

In 1959 Richard Feynman gave a seminal lecture at the California Institute of Technology [2], which sparked a new branch of science, namely quantum information technology. Since then many scientists have studied quantum mechanics to show how, by utilization of some extraordinary properties of nanoscale world (quantum superposition, interference or entanglement), it could be possible to perform tasks that are beyond capabilities of standard computers. And today, not even six decades later, engineers seem to be on the verge of constructing a full-fledged quantum devices, that could, if not revolutionize, then at least significantly enhance the computer technology [3, 4, 5, 6, 7, 8, 9].

Obviously, the transition from the classical computer science towards quantum information technology is not straightforward. Apart from the technical obstacles in building quantum computers (like the fragility of quantum states, that rapidly decohere upon interaction with

the environment), the construction of quantum algorithms is completely different from the development of classical algorithms. For this reason, it is not easy to translate existing classical algorithms in the way, that they could take the advantage of quantum properties. Therefore, investigation and development of new applications of quantum algorithms for solution of everyday problems is important for understanding the full potential of quantum computing and quantum information processing.

Quantum walks are one of highly studied models of quantum computation. They were inspired by the classical random walks which are widely used for simulation of some natural and social processes in physics, biology and even economics [10, 11]. It has been shown that quantum walks can benefit from the quantum phenomena to achieve quadratic [12] (or even exponential in some special cases [13]) speedup over their classical counterparts for some particular problems. Therefore it seems reasonable to explore this branch of quantum computation in the quest for new, better algorithms.

This thesis attempts to harness the quantum random walks, to perform image segmentation. The image segmentation, as a basic image processing tool, has a broad range of applications: from very trendy in recent years computer vision (object detection and recognition) [14, 15] to medical diagnostics and treatment planning [16, 17]. Research in this area could result in development of a novel method for solution of a practical everyday tasks as well as would give an insight into the properties and applicability of quantum walks.

1.2 Motivation

Image segmentation is used for solution of everyday problems. It is one of the first steps in image analysis tasks, since it allows for simplifying the input picture, which helps to save computational resources and enhance further processing. Segmentation is a very well known concept and there have been developed plenty of various algorithms for performing this task.

One of those methods is a very interesting algorithm presented by Grady in 2006 [1]. The author proposes performing image segmentation using classical random walks. User defines a set of seeds, pixels which have already assigned labels corresponding to the image segments. The algorithm then tries to determine for each unmarked pixel, what are the probabilities of reaching each seed as the first by a random walk staring from given pixel. Each pixel is then

assigned with a label of the seed that is most probable to be visited first by the walker.

Taking into consideration promising results obtained by Grady and bearing in mind the advantage of quantum walks over their classical counterparts, author of this thesis pose a question whether it is possible to harness quantum walk to perform image segmentation and perhaps, by utilizing those remarkable properties of quantum world, improve the classical solution. Guided by this motivation the author of this work conducted a scientific project to find an algorithm for performing image segmentation using quantum random walks.

1.3 Goals

The main goal of this thesis was to investigate the applicability of quantum walks for image segmentation. In order to achieve this aim several steps should have been undertaken:

- Research in the field of quantum walks – quantum computations is still quite niche area of research; also it is significantly different from the classical way of programing. Therefore, any work on the project had to be preceded by an extensive familiarization with principals of quantum computing and quantum walks.
- Quantum walk model development – as will be shown in chapter 2 quantum walks exist in two main kinds: discrete time and continuous time. Both types have different construction and properties, so the choice had to be considered and appropriate model had to be selected and built.
- Elaboration of an algorithm – after construction of the quantum walk model there had to be determined a way to obtain the image segmentation using the results of the walks.
- Implementation and simulation of the algorithm – since quantum computers are not yet accessible for academic use, quantum algorithms must have been tested using simulations of quantum processes running on a classical device.

1.4 Related work

The two constituent parts of this thesis are image segmentation and quantum walks. Currently, there are no references in the literature indicating any research concerning this combination.

1.4.1 Image segmentation methods

Image segmentation, as an extensively used image processing tool, has been carefully studied and there has been developed a multitude of different solutions. These methods can be grouped into few main categories [18, 19, 20].

One of the simplest classes contains threshold-based algorithms, which assign a label to each pixel according to its intensity value in comparison to one or more thresholds (depending on the desired number of segments to obtain). A very frequently used method of this kind is Otsu algorithm [21], which focuses on maximizing the difference of variances between segments. It gives satisfactory results if the segments cover areas of similar size, their variances are quite small and gaps between their peaks are considerable. Also, due to the fact that pixel location in the image is ignored these methods might yield an incoherent segmentation. Despite many limitations, threshold-based methods are praised for their simplicity and computational effectiveness.

Another approach that has been successfully applied to the image segmentation problem is based on clustering. It determines segments by aggregating pixels in groups (clusters) according to chosen metric. k-means method is one of available solutions [22]. It iteratively creates k clusters improving the division by moving the clusters center to the mean of all its members and reassigns elements to the clusters. Although this approach is a bit inefficient, as there needs to be processed whole image in each iteration, it is quite simple. The disadvantage is problem with choice of good initial settings (the number of clusters and initial cluster centers locations).

The image segmentation can be also achieved by utilizing tools designed for accomplishing a similar task of edge detection in the analyzed image [23]. Most often these methods perform image differentiation in order to determine gradient direction. They complete the task by applying various operators, like Sobel [24] of Laplace [25] operators. Transition from edge

detection to image segmentation is almost straightforward – it requires only assigning obtained regions with appropriate label.

The most interesting class, from the point of view of this thesis, are graph partitioning methods. These are effective tools as they take into consideration the neighborhood of the pixel by transforming the image into a weighted graph in which the weights of the edges are defined by the similarity of the neighboring pixels. To this category belong methods like: normalized cuts [26], interactive graph cuts [27], intelligent scissors [28], isoperimetric partitioning [29] and random walks [1].

The last mentioned approaches are very popular in recent years deep learning and neural networks, especially convolutional neural networks, which proved to be very successful in various image processing tasks. They have also found an application for image segmentation [30, 31, 32, 33]. The main issue with this kind of approach is long learning process and the need for a vast and diverse dataset of training samples. But, after developing a solid model, processing of new images is very fast. Those methods give much freedom and allow for construction of very complex and robust solutions.

There are by far much more studies and developed methods concerning image segmentation. Each of them expresses some benefits and possesses some limitations. It is a difficult task to invent a solution that would work well in every case, therefore there appear also some hybrid methods trying to exploit strengths of various solutions [34].

1.4.2 Quantum walks application

Nevertheless, the main goal of this thesis was not to improve the currently known algorithms for image segmentation, but to investigate the feasibility and development a method for performing segmentation using quantum random walks.

Since Nayak and Vishwanath [35] showed that quantum walks on line spread quadratically faster than their classical analogues, the quantum model has been studied to find algorithms that would allow for similar speedup [36]. The most spectacular achievement in this field was presented by Childs [12, 13]. The author considers a graph formed of two binary trees of height d that have their leaves glued together. He uses continuous time quantum walk starting from the root of one tree and proceeding towards the other one. Author proves that it takes for

the proposed algorithm $O(d^2)$ steps to find the opposite root with certain probability, while any classical solution would require $O(2^d)$ steps, hence he managed to achieve exponential speedup.

Quantum random walks have been used to construct various search algorithms. One of the most famous quantum algorithms is the Grover algorithm [37] that performs search for a marked element in an unordered database of size N. The algorithm requires only $O(\sqrt{N})$ queries to the database, which is quadratically less than in a classical solution. However, if the database is realized on a graph and the longest path between two elements is M then the total running time of the algorithm is $O(M\sqrt{N})$ (because between consecutive queries the algorithm might need to travel by M to the next element), which is not yet so spectacular [36].

This observation prompted scientists to elaborate algorithms that would perform search more effectively in terms of the movement on the graph. Shenvi et al. [38] proposed an algorithm that would search for an element in a boolean hypercube in time $O(\sqrt{N})$ (in comparison Grover algorithm would require $O(\sqrt{N}\log N)$ steps). Ambainis at al. [39] proposed discrete time quantum walk based algorithm for performing search in d-dimensional grid of size $N^{\frac{1}{d}} \times N^{\frac{1}{d}} \times ... \times N^{\frac{1}{d}}$ with complexity of $O(\sqrt{N}\log N)$ for two and $O(\sqrt{N})$ for three or more dimensions. Another examples of quantum walk based search algorithms were proposed by Szegedy [40] and Magniez et al. [41].

As far as non-search applications are concerned, Ambainis [42] developed also an algorithm for determining whether there are two identical values in a set of N elements that requires $O(N^{\frac{2}{3}})$ steps. And as a generalization $O(N^{\frac{k}{k+1}})$ if k elements with a given property are sought [42, 43]. Another example of application is quantum walk based image encryption [44].

Over the recent years there have been developed many various algorithms utilizing quantum walks. Most of the works consider rather theoretical problems, therefore it might be beneficial to elaborate an algorithm that would directly solve a practical, commonly used task.

1.5 Structure of the work

The document has been divided into six chapters, which cover following topics. Chapter 2 delves into theory concerning quantum walks and their classical analogues – classical random

walks. There is presented classification and anatomy of these computational models as well as examples that illustrate their properties. In chapter 3 there is delineated the task of image segmentation and are discussed challenges that emerged during the work on this project. Chapter 4 proposes three algorithms for accomplishing image segmentation with utilization of quantum walks. In chapter 5 has been included results of performed simulations of elaborated solutions as well as a discussion concerning the properties of these methods. Last chapter, 6, summarizes the effort put in the work on this project and draws conclusions on the questions posed during the formulation the topic of this thesis.

Chapter 2

Quantum random walks

This chapter provides an overview on the main domain of the work – quantum random walks. It discusses the theory, defines necessary concepts and provides illustrative examples. The actual description of quantum walks is preceded with an introduction of classical random walks in section 2.1. Then, in section 2.2, there are discussed quantum walks. Finally, both models are compared in section 2.3.

2.1 Classical random walks

Any discussion on quantum walks cannot be started without a brief introduction to their predecessors, classical random walks, which served also as an inspiration for its quantum counterparts. Gaining knowledge of the classical model should be beneficial for understanding of quantum walks, specifically their construction, behavior and properties.

2.1.1 Basic concepts and definitions

The term *random walks* was introduced by Karl Pearson at the beginning of the previous century [45]. He considered the following model: a man begins his journey at a starting point facing any direction, then walks an arbitrary number of steps straight ahead and turns by any angle. The man repeats this activity several times. Pearson was interested in calculating the

probability of finding the man at given distance from the starting point at the end of the walk. Failing to find a solution, he asked his readers for help.

Using more formal language and more general assumptions we can formulate a definition for the random walks:

Definition 1. *[46] Classical **random walk** is a stochastic process, during which a particle (walker) explores the space by randomly jumping from the current position to a neighboring one, based solely on the current state and according to the transition probabilities given at that state.*

Any random walk consists of two main components: *probability distribution* $\vec{p}_t$ and *transition matrix* M, which are defined as follows:

Definition 2. *[47] Let n be the size of the position space, then* $\vec{p}_t \in \mathbb{R}^n$ *denotes a **probability distribution** over position space of finding the walker at given position after t steps.*

Definition 3. *[47] Let n be the size of the position space, then* $M_{ij} \in \mathbb{R}^{n\times n}$ *is a **transition matrix** determining the probability of movement of the walker from position i to position j in a single step. M satisfies following constraints:*

$$\begin{aligned} 0 \leq M_{ij} \leq 1, \quad & \forall i,j \in \{0,1,2,...,n-1\}, \\ \sum_i M_{ij} = 1, \quad & \forall j \in \{0,1,2,...,n-1\}. \end{aligned} \tag{2.1}$$

If the transition matrix is constant over time the random walk can be described as a *Markov chain*, since it satisfies the Markov property of memoryless, *i.e.* its behavior is dependent only on the current state [46].

Markov chains (and therefore random walks), provided they are irreducible (each state is reachable form every other one) and aperiodic (this means each state has period equal to 1; *period* of given state is calculated as greatest common divisor of lengths of paths returning to that state), converge to a unique stationary distribution $\vec{\pi}$, which is independent of the initial distribution.

Definition 4. *[47] Probability distribution* $\vec{\pi}$ *of a Markov chain is called a **stationary distribution**, if it remains constant as the time progresses. In other words stationary*

distribution fulfills following condition:

$$\vec{\pi} = M\vec{\pi}. \tag{2.2}$$

Thus, if such random walker runs long enough, it will eventually lose all memory of where it has started. But it is not a case for quantum walks, as it will be discussed later in this work.

2.1.2 Random walk classification

Random walks are distinguished based on types of space and time in which they occur:

Space-based classification

Random walk can be preformed in various kinds of spaces and according to this we distinguish two main types of walk:

- Discrete space random walk – the set of available walker positions is well defined, in a form of a lattice or any other graph, which can be either finite of unbounded (like an axis of integers).
- Continuous space random walk – the walker can be placed at any coordinates of the position space. Good example here is the Pearson case, where the man (after sufficient number of steps) can reach every point in the two dimensional space.

This work focused entirely on the former case.

Time-based classification

Separate approach for categorization of walks is based on the continuousness of time at which the transitions occur:

- discrete time random walks – there is a constant unit of time that separates consecutive steps, so the states that the walker is in over time can be indexed with integer numbers.

The discrete time random walk can be described by the equation:

$$\vec{p}_t = M\vec{p}_{t-1}, \tag{2.3}$$

or alternatively:

$$\vec{p}_t = M^t\vec{p}_0. \tag{2.4}$$

- continuous time random walk – the walker step can occur at any time according to the parameter γ describing the probability of transition per unit of time. Now, changing slightly the denotation of probability distribution to $\vec{p}(t)$, the walk formula takes the form of differential equation:

$$\frac{d\vec{p}(t)}{dt} = \gamma M\vec{p}(t-1). \tag{2.5}$$

which after solving gives following relationship:

$$\vec{p}(t) = e^{\gamma Mt}\vec{p}(0). \tag{2.6}$$

2.1.3 Measuring the performance

One of the most important qualities of the random walk is its performance, i.e. how prone it is to explore the space of states. In order to qualify and compare different walk models there have been developed several metrics for measuring random walks on graph [47]:

- Hitting time (H_{ij}) – expected number of steps that takes the walker to reach node j starting from node i.
- Commute time ($k(i,j)$) – expected number of steps required for a walk starting at node i to return to i via j:

$$k(i,j) = H_{ij} + H_{ji}. \tag{2.7}$$

- Mixing time (M_ε) – number of steps after which the walk distribution is ε-close to the

stationary distribution, provided it converges to one:

$$M_\varepsilon = \min\{T | \forall t \geq T : \|\vec{p}_t - \vec{\pi}\| \leq \varepsilon\}. \tag{2.8}$$

- Mixing rate ($\frac{1}{M_\varepsilon}$) – measure how fast the discrete random walk converges to its stationary distribution.

2.1.4 Example – random walk on an infinite line

As a visualization of above considerations one can imagine a simple example of a random walk: an infinite axis of integers and a particle starting at position $x_0 = 0$. Upon each step the particle moves left or right with equal probability (e.g. the direction can be drawn by a coin toss: heads means step the position with index smaller than current by one, tails - step to higher index) as visualized on figure 2.1. After first step the walker would be found at positions -1 or +1 with probability 50%, after next step it would end up at position 0 with probability 50% or at position -2 or +2 with probability 25%, etc. This is illustrated on the figures 2.2, which shows probabilities of walker reaching given position in exactly 8 and 9 steps. Figure 2.3 shows the distribution after 100 steps.

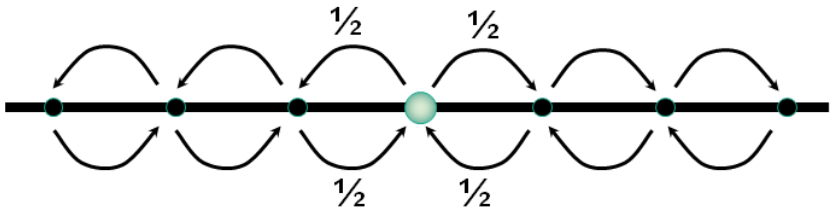

Figure 2.1: Walk on infinite line – a particle (green dot) at each time step moves either left or right with equal transition probabilities.

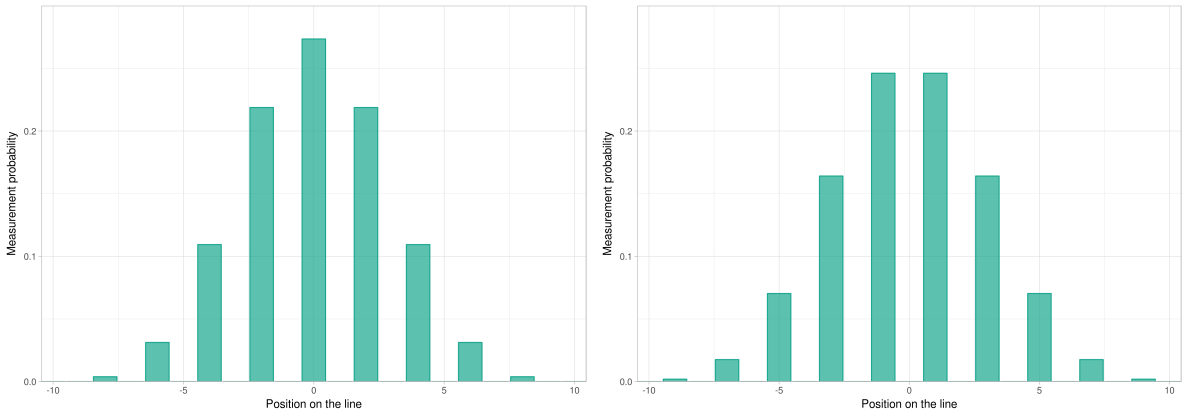

(a) **(b)**

Figure 2.2: Probability of finding the particle at given position after: 2.2a 8 and 2.2b 9 steps of discrete time classical walk.

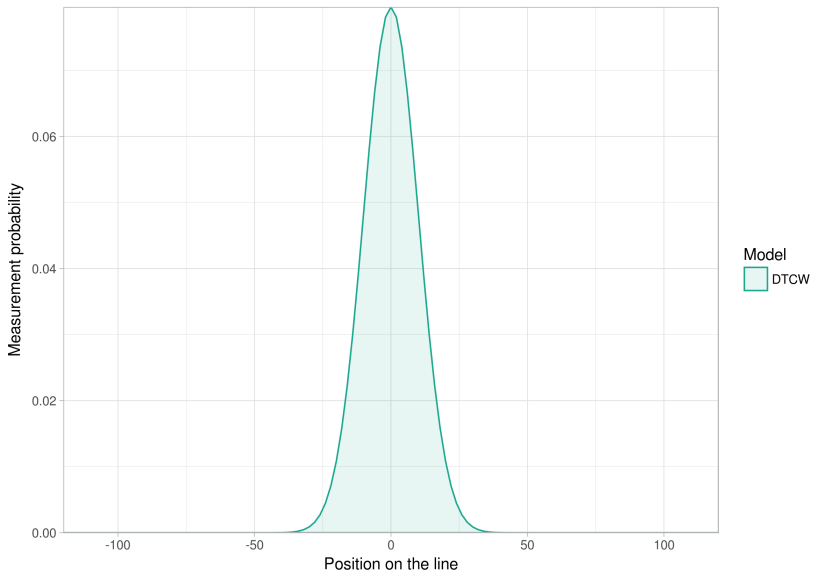

Figure 2.3: Probability distribution of finding the particle at given position after 100 steps of discrete time classical walk. The zero probabilities at odd positions are ignored.

This trivial illustration allows for observation of a few interesting properties:

- the walker oscillates around its starting position,
- after t steps the walker can be found at positions $[x_0 - t; x_0 + t]$,
- after even (odd) number of steps the particle has non-zero probability of ending up at positions distant from the starting point by even (odd) number of steps,
- the described graph is a bipartite graph (each edge has one end in an even index and the other in an odd one), so is not aperiodic, and therefore the walk does not converge to a stationary distribution,
- despite that it can be noticed that after t steps the probability distribution is close to a Gaussian distribution with a standard deviation of the order of $O(\sqrt{t})$.

2.2 Quantum random walks

Bearing in mind the success of the random walks in development of many efficient algorithms, it seemed reasonable to make an attempt to harness their quantum counterparts in construction of even more powerful algorithms, thanks to utilization of some remarkable properties of the quantum world. First work on *quantum random walks* (or shortly *quantum walks*) was published by Aharonov in 1993 [48], so this is a relatively new research area. The main goals of work in this field, apart from exploring the quantum walks as such, are studying the connection between classical and quantum walks and designing appropriate and universal methods of measuring and quantifying the performance and properties of the quantum walks.

Similarly to the classical approach, the quantum walks can be classified based on the continuousness of space and time. In this section there will be discussed two types of quantum walks: discrete time and continuous time quantum walks. As it will be shown, their nature is more complex than it is observed in the case of classical random walks and there are hardly any explicit similarities between those two models.

2.2.1 Discrete time quantum walks

Subsystems

Unlike the classical discrete time random walk, where the walker state is described solely by its position, the state of discrete time quantum walk on graph consists of two subsystems:

- Position space $\mathscr{H}_p$ – a Hilbert space spanned by canonical basis vectors $|i\rangle_p$ for each achievable walker position i (each vertex of the graph is labeled with consecutive integer number i). Then the walker position state is described as follows:

$$\begin{aligned} |\psi\rangle_p &= \sum_i a_i |i\rangle_p, \\ \sum_i \|a_i\|^2 &= 1. \end{aligned} \tag{2.9}$$

- Coin space $\mathscr{H}_c$ – apart from the standard position space the discrete time quantum walks possess additional subsystem named coin space, which determines direction of the walker in the position space at each time step. The dimensionality of the coin space depends on the number of possible moves of the particle: e.g. on the line there are two options, namely left or right, on a lattice there are four, and for an arbitrary graph it is determined by the degree of its vertices.

The complete state of the quantum walk is of the following form:

$$|\psi\rangle = |\psi\rangle_p \otimes |\psi\rangle_c, \quad |\psi\rangle \in \mathscr{H}_p \otimes \mathscr{H}_c. \tag{2.10}$$

Evolution operators

The discrete time quantum walk is conducted in the way, that at each time step two operators – coin operator and shift operator are applied to current walker state to perform transition:

- Coin operator – it works similarly to tossing a coin, but is deterministic. This means that knowing the current state of the coin subsystem and the coin operator, one can exactly tell what would be outcome of the operation. There are two distinguished kinds of discrete time quantum walks based on the type of coin operator:

– Homogeneous discrete time quantum walk – the coin operator is independent of the position state and constant during the whole walk, it takes the form:

$$C = \mathbb{1}_p \otimes C', \tag{2.11}$$

where $\mathbb{1}_p$ is an identity operator acting on the position subsystem (therefore leaving it unchanged) and C' is the constant operator transforming the coin subsystem.

– Inhomogeneous discrete time quantum walk – in this case the coin operator varies according to the current position of the particle:

$$C = \sum_i (|i\rangle_p \langle i|_p \otimes C_i). \tag{2.12}$$

The expression $\sum_i |i\rangle_p \langle i|_p$ is equal to the identity operator $\mathbb{1}_p$, so it does not alter the position space, but by using projection operator $|i\rangle_p \langle i|_p$ the appropriate C_i operator is applied to the coin subsystem according to the current walker position.

- Shift operator – upon this operator the walker moves (changes its position) in direction indicated by the current state of the coin subsystem. General form of the shift operator for the walk on the graph can be formulated as follows:

$$S = \sum_i \sum_{j=1}^{d_i} |v(i,j)\rangle_p \langle i|_p \otimes |j\rangle_c \langle j|_c, \tag{2.13}$$

where d_i is the degree of node i and $v(i,j)$ denotes the neighbor of i connected with its j-th edge (for some arbitrary edge labeling). Again $\sum_{j=1}^{d_i} |j\rangle_c \langle j|_c$ has no effect on the coin subsystem, but together with $|v(i,j)\rangle_p \langle i|_p$ allows to perform the right move according to the state of the walker.

At each step of the walk there is applied the coin operator followed tightly by the shift operator. So, in order to shorten the notation, the two operators can be combined into one operator U:

$$U = SC. \tag{2.14}$$

Operators are represented as square matrices with the same size as the space they act on. Like every operation in the quantum computation world, the above operators need to be reversible. This is ensured by using only *unitary operators*.

Definition 5. *[49] An operator U is an **unitary operator** if it satisfies the following condition:*

$$UU^\dagger = U^\dagger U = \mathbb{1}, \tag{2.15}$$

where $U^\dagger$ denotes the Hermitian conjugate of the operator U.

Formula

Given the initial state of the subsystems $|\psi_0\rangle = |\psi_0\rangle_p \otimes |\psi_0\rangle_c$ and evolution operator $U = SC$, the discrete time quantum walk can be described by the equation:

$$|\psi_t\rangle = U^t |\psi_0\rangle. \tag{2.16}$$

And a single step has following form:

$$|\psi_t\rangle = U|\psi_{t-1}\rangle. \tag{2.17}$$

Notice, that the above formulas are exactly the same as for the classical discrete time quantum walks.

Limiting distribution

As it was mentioned earlier, the quantum processes do not converge to a stationary distribution:

Lemma 1. *Because of unitarity of evolution operators, quantum Markov chain does not converge to a stationary distribution, unless its evolution operator is an identity operator.*

Proof. The substantial property of an unitary operator U is that it preserves the norm of a vector $|\psi\rangle$ it is applied to:

$$\|U|\psi\rangle\| = \||\psi\rangle\|. \tag{2.18}$$

The unitary operator also preserves the norm of the difference of subsequent state vectors:

$$\||\psi_{t+1}\rangle - |\psi_t\rangle\| = \|U|\psi_t\rangle - U|\psi_{t-1}\rangle\| = \|U(|\psi_t\rangle - |\psi_{t-1}\rangle)\| = \||\psi_t\rangle - |\psi_{t-1}\rangle\|. \quad (2.19)$$

If there was a quantum Markov chain $|\phi_0\rangle, |\phi_1\rangle, ...$, that would converge to a stationary distribution $|\pi\rangle$, then:

$$\lim_{t\to\infty} \||\phi_{t+1}\rangle - |\phi_t\rangle\| = \|U|\pi\rangle - |\pi\rangle\| = \||\pi\rangle - |\pi\rangle\| = 0. \quad (2.20)$$

The norm of a vector is zero only if this is a zero vector. This would imply that all states of the quantum Markov chain would be the same, therefore the evolution operator would have to be an identity. ■

Since the quantum random walks do not converge, the notion of *stationary distribution* cannot be used during analysis of these walks. It was proposed by Aharonov et al. [49] to consider *average distribution* and *limiting distribution* instead.

Definition 6. *[49] Consider the probability distribution $\vec{P}_t(|\psi_0\rangle)$ on the nodes of the graph after t steps of quantum walk starting from the initial state $|\psi_0\rangle$:*

$$P_t^i(|\psi_0\rangle) = \sum_j \|(\langle i|_p \otimes \langle j|_c)|\psi_t\rangle\|^2. \quad (2.21)$$

*Then the **average distribution** $\overline{P}_T(|\psi_0\rangle)$ is the mean over the distributions in each time step until T:*

$$\overline{P}_T(|\psi_0\rangle) = \frac{1}{T}\sum_{t=0}^{T-1} \vec{P}_t(|\psi_0\rangle). \quad (2.22)$$

Notice that the *average distribution* can be understood as a measure of how long the quantum walker spends at each of the position states throughout the first T steps of the walk.

It was shown in [49] that, for any initial state $|\psi_0\rangle$, the average distribution converges as the time approaches infinity and the limit is denoted as *limiting distribution*.

Definition 7. *[49] **Limiting distribution** of the quantum random walk starting from the initial state $|\psi_0\rangle$:*

$$\vec{\pi}(|\psi_0\rangle) = \lim_{T\to\infty} \overline{P}_T(|\psi_0\rangle). \quad (2.23)$$

The *limiting distribution* is not unique, but depends on the initial state.

The definition of *limiting distribution* allows to restate the notion of *mixing time* for the quantum case:

Definition 8. *[49]* ***Mixing time****, M_ε, of a quantum Markov chain is calculated as number of steps required for the average distribution to be ε-close to the limiting distribution, starting from any basis state:*

$$M_\varepsilon = \min\{T | \forall t \geq T, |\psi_0\rangle = |i\rangle_p \otimes |j\rangle_c : \|\overline{P}_t(|\psi_0\rangle) - \vec{\pi}(|\psi_0\rangle)\| \leq \varepsilon\}. \tag{2.24}$$

2.2.2 Example – discrete time quantum walk on an infinite line

Consider the analogous example to the one discussed at the end of the previous section and illustrated in figure 2.1: quantum walk on an infinite line with a particle starting at the position 0 with the ability to move either left or right. More formally:

- Position space $\mathscr{H}_p$ with the basis states $\{...,|-2\rangle_p,|-1\rangle_p,|0\rangle_p,|1\rangle_p,|2\rangle_p,...\}$,
- Coin space $\mathscr{H}_c$ with two basis states $\{|\leftarrow\rangle_c,|\rightarrow\rangle_c\}$,
- Shift operator S takes simplified form of the equation 2.13:

$$S = \sum_i (|i-1\rangle_p\langle i|_p \otimes |\leftarrow\rangle_c\langle\leftarrow|_c + |i+1\rangle_p\langle i|_p \otimes |\rightarrow\rangle_c\langle\rightarrow|_c), \tag{2.25}$$

- Coin operator $C = \mathbb{1}_p \otimes C'$ – where C' can be any $2x2$ unitary operator. The choice of this operator has a tremendous influence on the behavior of the quantum walk. In this example there will be presented, extensively used in the world of quantum walks, Hadamard operator H:

$$H = \frac{1}{\sqrt{2}}\begin{bmatrix} 1 & 1 \\ 1 & -1 \end{bmatrix}. \tag{2.26}$$

  This is a simple, yet very interesting operator, since it introduces quantum superposition

upon application to a basis state:

$$H|\leftarrow\rangle_c = \frac{|\leftarrow\rangle_c + |\rightarrow\rangle_c}{\sqrt{2}},$$
$$H|\rightarrow\rangle_c = \frac{|\leftarrow\rangle_c - |\rightarrow\rangle_c}{\sqrt{2}}. \tag{2.27}$$

The last choice is the selection of the initial state. As the walker starts at the position 0 the initial state of position subsystem is $|0\rangle_p$. In this example, there will be shown how significantly the change in the initial state of the coin impacts the behavior of the walk.

Walk 1.

Consider an initial coin state as a basis state $|\leftarrow\rangle_c$. Then the initial state of the walk takes form: $|\psi_0\rangle = |0\rangle_p \otimes |\leftarrow\rangle_c$. The table 2.1 shows first five steps of this walk: the states of the systems after successive application of operator $U = SC$ and associated with them probabilities of measuring the particle at given positions. At first, the walker seems to behave exactly like in the classical model, but after third step there begins to form a skewness towards the negative positions. Also starting from the fifth step there appear two peeks at both ends of the distribution, while in the center (positions around 0) the distribution is almost uniform and the probability of finding the walker there is quite low. This can be clearly seen in the figure 2.4 presenting the probability distributions of finding the walker at given position after 100 steps.

Time step	**Walker state**	**Probabilities of finding walker at position**										
		-5	-4	-3	-2	-1	0	1	2	3	4	5
0	$\|0\rangle_p \otimes \|\leftarrow\rangle_c$						1					
1	$\frac{1}{\sqrt{2}}(\|-1\rangle_p \otimes \|\leftarrow\rangle_c + \|1\rangle_p \otimes \|\rightarrow\rangle_c)$					$\frac{1}{2}$		$\frac{1}{2}$				
2	$\frac{1}{2}(\|-2\rangle_p \otimes \|\leftarrow\rangle_c + \|0\rangle_p \otimes \|\rightarrow\rangle_c +$ $+\|0\rangle_p \otimes \|\leftarrow\rangle_c) - \|2\rangle_p \otimes \|\rightarrow\rangle_c)$				$\frac{1}{4}$		$\frac{1}{2}$		$\frac{1}{4}$			
3	$\frac{1}{2\sqrt{2}}(\|-3\rangle_p \otimes \|\leftarrow\rangle_c + \|-1\rangle_p \otimes \|\rightarrow\rangle_c +$ $+2\|-1\rangle_p \otimes \|\leftarrow\rangle_c - \|1\rangle_p \otimes \|\leftarrow\rangle_c + \|3\rangle_p \otimes \|\rightarrow\rangle_c)$			$\frac{1}{8}$		$\frac{5}{8}$		$\frac{1}{8}$		$\frac{1}{8}$		
4	$\frac{1}{4}(\|-4\rangle_p \otimes \|\leftarrow\rangle_c + \|-2\rangle_p \otimes \|\rightarrow\rangle_c +$ $+3\|-2\rangle_p \otimes \|\leftarrow\rangle_c + \|0\rangle_p \otimes \|\rightarrow\rangle_c - \|0\rangle_p \otimes \|\leftarrow\rangle_c -$ $-\|2\rangle_p \otimes \|\rightarrow\rangle_c + \|2\rangle_p \otimes \|\leftarrow\rangle_c - \|4\rangle_p \otimes \|\rightarrow\rangle_c)$		$\frac{1}{16}$		$\frac{5}{8}$		$\frac{1}{8}$		$\frac{1}{8}$		$\frac{1}{16}$	
5	$\frac{1}{4\sqrt{2}}(\|-5\rangle_p \otimes \|\leftarrow\rangle_c + \|-3\rangle_p \otimes \|\rightarrow\rangle_c +$ $+4\|-3\rangle_p \otimes \|\leftarrow\rangle_c + 2\|-1\rangle_p \otimes \|\rightarrow\rangle_c - 2\|1\rangle_p \otimes \|\rightarrow\rangle_c +$ $+2\|3\rangle_p \otimes \|\rightarrow\rangle_c - \|3\rangle_p \otimes \|\leftarrow\rangle_c + \|5\rangle_p \otimes \|\rightarrow\rangle_c)$	$\frac{1}{32}$		$\frac{17}{32}$		$\frac{1}{8}$		$\frac{1}{8}$		$\frac{5}{32}$		$\frac{1}{32}$

Table 2.1: First few states of discrete time quantum walk on an infinite line with Hadamard coin starting from an initial state $|0\rangle_p \otimes |\leftarrow\rangle_c$ and related to them probabilities of finding particle at given position after measurement (blank cells exhibit 0 probability).

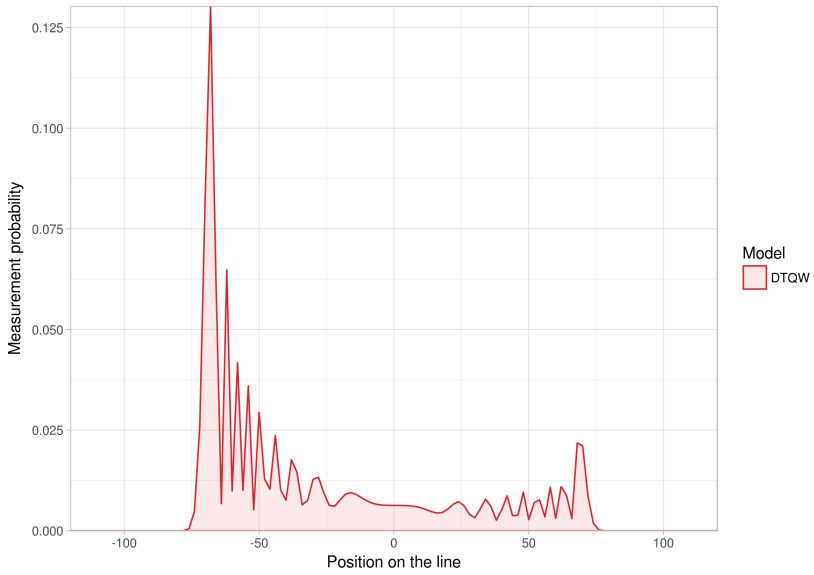

Figure 2.4: Probability distribution over the position space of finding the walker at given position after 100 steps of discrete time quantum walk on an infinite line with Hadamard coin starting from an initial state $|\psi_0\rangle = |0\rangle_p \otimes |\leftarrow\rangle_c$.

Walk 2.

Consider exactly the same walk model as in the previous example, but facing the opposite direction – the initial coin state is now the other basis state, $|\rightarrow\rangle_c$. Now the initial state takes form: $|\psi_0\rangle = |0\rangle_p \otimes |\rightarrow\rangle_c$. The table 2.2 and figure 2.5 illustrate the behavior of the walk. As it could be predicted the walk behavior and the distribution of the walk is symmetrical to the first case.

Time step	**Walker state**	**Probabilities of finding walker at position**										
		-5	-4	-3	-2	-1	0	1	2	3	4	5
0	$\|0\rangle_p \otimes \|\rightarrow\rangle_c$						1					
1	$\frac{1}{\sqrt{2}}(\|-1\rangle_p \otimes \|\leftarrow\rangle_c - \|1\rangle_p \otimes \|\rightarrow\rangle_c)$					$\frac{1}{2}$		$\frac{1}{2}$				
2	$\frac{1}{2}(\|-2\rangle_p \otimes \|\leftarrow\rangle_c + \|0\rangle_p \otimes \|\rightarrow\rangle_c -$ $-\|0\rangle_p \otimes \|\leftarrow\rangle_c + \|2\rangle_p \otimes \|\rightarrow\rangle_c)$				$\frac{1}{4}$		$\frac{1}{2}$		$\frac{1}{4}$			
3	$\frac{1}{2\sqrt{2}}(\|-3\rangle_p \otimes \|\leftarrow\rangle_c + \|-1\rangle_p \otimes \|\rightarrow\rangle_c -$ $-2\|1\rangle_p \otimes \|\rightarrow\rangle_c + \|1\rangle_p \otimes \|\leftarrow\rangle_c - \|3\rangle_p \otimes \|\rightarrow\rangle_c)$			$\frac{1}{8}$		$\frac{1}{8}$		$\frac{5}{8}$		$\frac{1}{8}$		
4	$\frac{1}{4}(\|-4\rangle_p \otimes \|\leftarrow\rangle_c + \|-2\rangle_p \otimes \|\rightarrow\rangle_c +$ $+\|-2\rangle_p \otimes \|\leftarrow\rangle_c - \|0\rangle_p \otimes \|\rightarrow\rangle_c - \|0\rangle_p \otimes \|\leftarrow\rangle_c +$ $+3\|2\rangle_p \otimes \|\rightarrow\rangle_c - \|2\rangle_p \otimes \|\leftarrow\rangle_c + \|4\rangle_p \otimes \|\rightarrow\rangle_c)$		$\frac{1}{16}$		$\frac{1}{8}$		$\frac{1}{8}$		$\frac{5}{8}$		$\frac{1}{16}$	
5	$\frac{1}{4\sqrt{2}}(\|-5\rangle_p \otimes \|\leftarrow\rangle_c + \|-3\rangle_p \otimes \|\rightarrow\rangle_c +$ $+2\|-3\rangle_p \otimes \|\leftarrow\rangle_c - 2\|-1\rangle_p \otimes \|\leftarrow\rangle_c + 2\|1\rangle_p \otimes \|\leftarrow\rangle_c -$ $-4\|3\rangle_p \otimes \|\rightarrow\rangle_c + \|3\rangle_p \otimes \|\leftarrow\rangle_c - \|5\rangle_p \otimes \|\rightarrow\rangle_c)$	$\frac{1}{32}$		$\frac{5}{32}$		$\frac{1}{8}$		$\frac{1}{8}$		$\frac{17}{32}$		$\frac{1}{32}$

Table 2.2: First few states of discrete time quantum walk on an infinite line with Hadamard coin starting from an initial state $|0\rangle_p \otimes |\rightarrow\rangle_c$ and related to them probabilities of finding particle at given position after measurement.

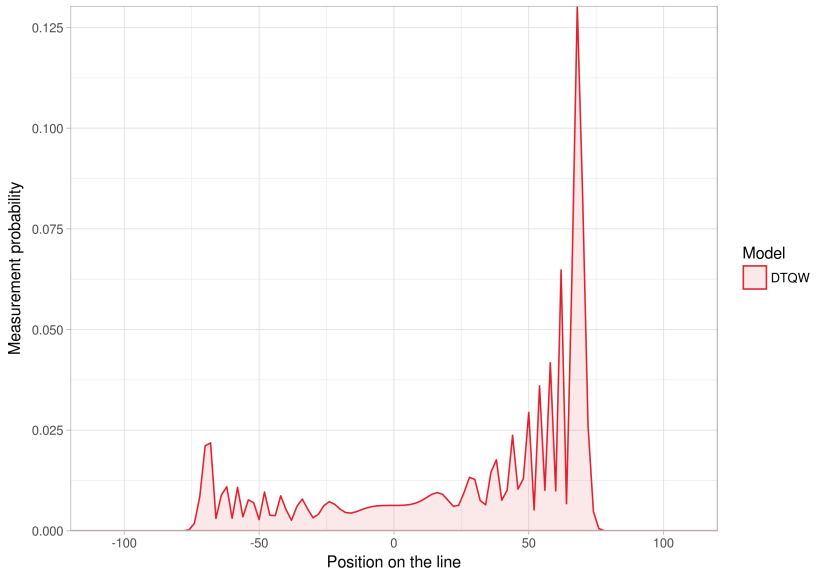

Figure 2.5: Probability distribution over the position space of finding the walker at given position after 100 steps of discrete time quantum walk on an infinite line with Hadamard coin starting from an initial state $|\psi_0\rangle = |0\rangle_p \otimes |\rightarrow\rangle_c$.

Walk 3.

Looking for a set up for the walk that would result in symmetrical behavior one could choose the following initial conditions: $|\psi_0\rangle = \frac{1}{\sqrt{2}}|0\rangle_p \otimes (|\leftarrow\rangle_c + |\rightarrow\rangle_c)$. In theory combining two complementary walks should give the desired result. But what exactly happens is:

$$|\psi_1\rangle = U|\psi_0\rangle = SC(\frac{1}{\sqrt{2}}|0\rangle_p \otimes (|\leftarrow\rangle_c + |\rightarrow\rangle_c)) = S(|0\rangle_p \otimes |\leftarrow\rangle_c) = |-1\rangle_p \otimes |\leftarrow\rangle_c. \quad (2.28)$$

The outcome is quite surprising - the state after the first step is almost identical as the initial state in the first example, only shifted by one position to the left. Further the walk would shape exactly like the first example starting from position -1. The thing that happens here is the quantum interference – parts of both walks that go left amplify each other, while the other components nullify. The reason for that is unequal effect of Hadamard operator on both basis states, caused by the -1 affecting only $|\rightarrow\rangle_c$ in the second equation in 2.27.

Walk 4.

A way to obtain a quantum walk that propagates equally in both directions is to set the initial state to: $|\psi_0\rangle = \frac{1}{\sqrt{2}}|0\rangle_p \otimes (|\leftarrow\rangle_c + i|\rightarrow\rangle_c)$. The only detail that distinguishes it form the previous case is the imaginary unit i. It works like a phase shift on one of the components, preventing them from interfering and nullifying the walk in one direction. Again, the table 2.3 analyzes first few steps of the walk, while the figure 2.6 presents it in its more advanced stage - after 100 steps. The distribution is symmetrical and with the shape as the sum of distributions shown in figures 2.4 and 2.5.

Another approach to construct a symmetrical quantum walk could be to use a coin operator that treats both basis states equally, e.g.:

$$Y = \frac{1}{\sqrt{2}} \begin{bmatrix} 1 & i \\ i & 1 \end{bmatrix}. \tag{2.29}$$

Time step	**Walker state**	**Probabilities of finding walker at position**								
		-4	-3	-2	-1	0	1	2	3	4
0	$\frac{1}{\sqrt{2}}\|0\rangle_p \otimes (\|\leftarrow\rangle_c + i\|\rightarrow\rangle_c)$					1				
1	$\frac{1}{2}((1+i)\|-1\rangle_p \otimes \|\leftarrow\rangle_c + (1-i)\|1\rangle_p \otimes \|\rightarrow\rangle_c)$				$\frac{1}{2}$		$\frac{1}{2}$			
2	$\frac{1}{2\sqrt{2}}((1+i)\|-2\rangle_p \otimes \|\leftarrow\rangle_c + (1+i)\|0\rangle_p \otimes \|\rightarrow\rangle_c +$ $+(1-i)\|0\rangle_p \otimes \|\leftarrow\rangle_c - (1-i)\|2\rangle_p \otimes \|\rightarrow\rangle_c)$			$\frac{1}{4}$		$\frac{1}{2}$		$\frac{1}{4}$		
3	$\frac{1}{4}((1+i)\|-3\rangle_p \otimes \|\leftarrow\rangle_c + (1+i)\|-1\rangle_p \otimes \|\rightarrow\rangle_c + 2\|-1\rangle_p \otimes \|\leftarrow\rangle_c -$ $-2i\|1\rangle_p \otimes \|\rightarrow\rangle_c - (1-i)\|1\rangle_p \otimes \|\leftarrow\rangle_c + (1-i)\|3\rangle_p \otimes \|\rightarrow\rangle_c)$		$\frac{1}{8}$		$\frac{3}{8}$		$\frac{3}{8}$		$\frac{1}{8}$	
4	$\frac{1}{4\sqrt{2}}((1+i)\|-4\rangle_p \otimes \|\leftarrow\rangle_c + (1+i)\|-2\rangle_p \otimes \|\rightarrow\rangle_c +$ $+(3+i)\|-2\rangle_p \otimes \|\leftarrow\rangle_c + (1-i)\|0\rangle_p \otimes \|\rightarrow\rangle_c - (1+i)\|0\rangle_p \otimes \|\leftarrow\rangle_c -$ $-(1-3i)\|2\rangle_p \otimes \|\rightarrow\rangle_c - (1-i)\|2\rangle_p \otimes \|\leftarrow\rangle_c + (1-i)\|4\rangle_p \otimes \|\rightarrow\rangle_c)$	$\frac{1}{16}$		$\frac{3}{8}$		$\frac{1}{8}$		$\frac{3}{8}$		$\frac{1}{16}$

Table 2.3: First few states of discrete time quantum walk on an infinite line with Hadamard coin starting from an initial state $\frac{1}{\sqrt{2}}|0\rangle_p \otimes (|\leftarrow\rangle_c + i|\rightarrow\rangle_c)$ and related to them probabilities of finding particle at given position after measurement.

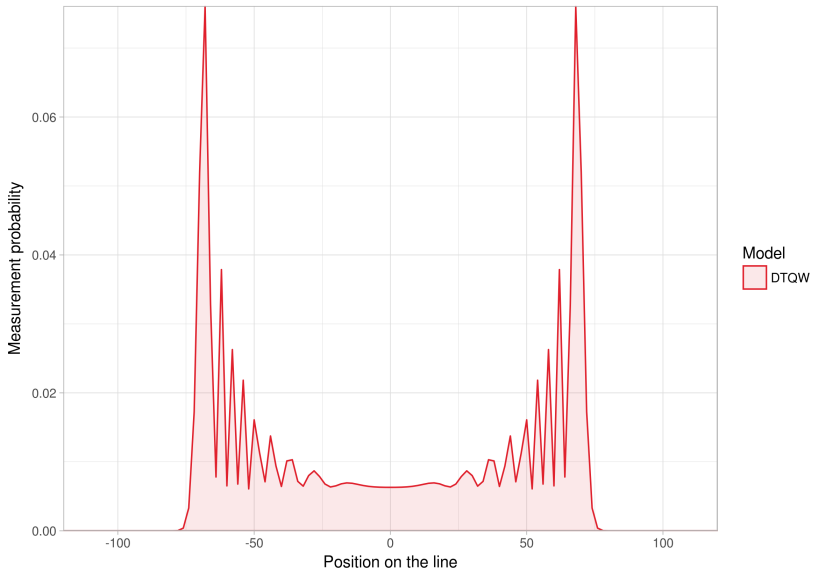

Figure 2.6: Probability distribution over the position space of finding the walker at given position after 100 steps of discrete time quantum walk on an infinite line with Hadamard coin starting from an initial state $\frac{1}{\sqrt{2}}|0\rangle_p \otimes (|\leftarrow\rangle_c + i|\rightarrow\rangle_c)$.

2.2.3 Continuous quantum walks

The continuous time model of quantum walk is significantly different from the discrete time quantum walk and more similar to its classical analogue. There is no coin used, only the position space is required. The transitions are not quantized into steps, but can occur at any time according to a time-independent constant γ, describing the jumping rate. This constant is used to construct a Hamiltonian matrix H, which in turn is a generator of the evolution operator $U(t)$:

$$U(t) = e^{-iHt}. \tag{2.30}$$

Finally, the continuous time quantum walk is described by the equation:

$$|\psi(t)\rangle = U(t)|\psi(0)\rangle. \tag{2.31}$$

In order to adhere to rules of quantum computation, the operator U has to be unitary:

Lemma 2. *If H is a Hermitian matrix (i.e. $H^\dagger = H$) and $t \in \mathbb{R}$, then matrix $U = e^{-iHt}$ is unitary.*

Proof. Utilizing directly properties of matrix exponential and Hermitian transpose:

$$U^\dagger U = (e^{-iHt})^\dagger e^{-iHt} = e^{(-iHt)^\dagger} e^{-iHt} = e^{\overline{(-it)} H^\dagger} e^{-iHt} = e^{iHt} e^{-iHt} = e^0 = \mathbb{1}. \tag{2.32}$$

■

So any Hermitian matrix of size of the position space can be used as a generator of continuous time quantum walk.

2.3 Comparison of classical and quantum walks

Although the equations governing both classical and quantum walks, at first glance, are almost identical, the mechanisms hidden underneath are significantly different. This section points out some constituent discrepancies between those two kinds of walks:

- quantum walker state can be a superposition of basis states,
- during quantum walk, the components of walker state can interfere, resulting in amplification or nullification of some of them,
- quantum evolution operator needs to be unitary, while the classical walk can utilize any stochastic matrix,
- quantum walk is reversible and does not converge to a stationary distribution, therefore it keeps the memory of where it has started, unlike the classical random walks,
- discrete time quantum walk utilizes additional coin subspace, responsible for indicating the direction of the walk,
- in classical random walk, the walker at each time step changes its position randomly, according to the transition probabilities at current state; in the case of quantum random walks, each step is deterministic and the randomness is introduced at the end of the process upon the measurement,

- based on the examples of random walks on a line, it can be seen how different can be the behavior of both counterparts; while the classical walk tends to stay close to its starting position, the quantum walker is more keen to explore the space cumulating the probability of occurrence at the end of the position range; figure 2.7 presents the comparison of probability distributions of discrete time classical and quantum walks starting from position 0 after 100 steps. Figure 2.8 performs similar comparison for continuous time models.

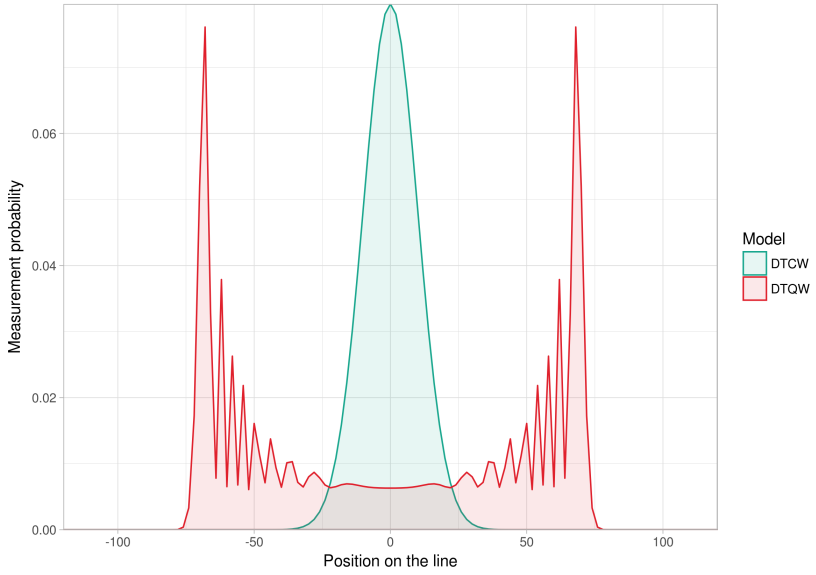

Figure 2.7: Comparison of discrete time classical (DTCW) and quantum (DTQW) walks on an infinite line after 100 steps. The zero probabilities at odd positions are ignored.

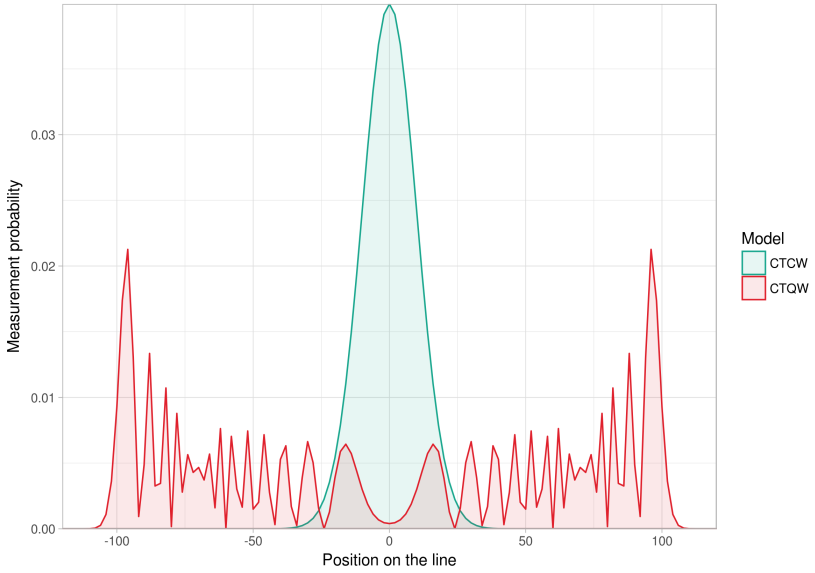

Figure 2.8: Comparison of continuous time classical (CTCW) and quantum (CTQW) walks on an infinite line after time $t = 100$, for $\gamma = 1$.

2.4 Summary

This chapter provided a brief introduction to the quantum computational models studied in this thesis. As the starting point for the discussion served random walks, which as the classical base for quantum walks share with them some fundamental assumptions and ideas. This allowed for a gentle and gradual transition towards quantum model. There were presented theoretical background, classification, important properties and construction details of quantum walks. Finally, there was described a simple example, which depicted the substantial differences of these two concepts.

Theory described in this chapter would allow for understanding the challenges (stated in the next chapter 3) that needed to be faced as well as the mechanisms of proposed solutions, included in chapter 4.

To summarize the theoretical discussion, over the years classical random walks have proved to be a very successful model and found a broad scope of applications. Quantum walks managed to outperform their classical counterparts even in some simple cases, like walk on

an infinite line. This prompts scientists, to seek solutions based on this computational model, however due to the extraordinary nature of quantum walks and quantum computation this is a very challenging quest.

Chapter 3

Problem outline

This chapter discusses issues raised in this thesis. It describes the problem of image segmentation, in section 3.1 and presents the main challenges the author had to face during the work on the project, in section 3.2, focusing on the most difficult one – construction of evolution operators, in section 3.3.

3.1 Image segmentation

Segmentation is a process of partitioning a greater whole into smaller parts. For example, in economics, there is a concept of market segmentation, which means dividing consumer market into groups of consumers that exhibit similar characteristics. In computer studies there are common notions of memory segmentation (partitioning computer memory into segments which are allocated to processes to operate on in order to enhance memory protection) or network segmentation (splitting network into subnetworks, which improves security as well as facilitates administration). *Image segmentation* process is not much different from those examples.

Definition 9. *[20]* ***Image segmentation*** *is a process of dividing entire image into multiple separate segments – areas inside which pixels expose the similar characteristics (e.g. intensity, hue, texture).*

Equivalently, *image segmentation* can be defined as an activity of assigning each pixel of an image with a label in the way that pixels sharing similar traits of interest are labeled alike.

This thesis focuses on a *seeded image segmentation*. It is a type of image segmentation, which takes as an input, apart from the image itself, a list of seeds - pixels which already have a label assigned. These seeds serve as starting points for the walk.

3.2 Challenges

In order to construct desired algorithm for image segmentations there were several elements that needed to be considered:

- converting the input image into an appropriate position space – the image had to be translated in graph, that would accurately express the image content,
- forming initial state for the walk/walks based on provided seeds,
- considering the choice of the quantum walk model to be harnessed – whether to use discrete time of continuous time quantum walks,
- constructing evaluation operators, that would induce the right quantum walk behavior – that would encourage the walker to explore regions of pixels with similar intensity. This was the hardest problem to solve, as it is described in the next section,
- performing quantum walk and gathering/measuring its outcome – applying the evolution operators and recording necessary elements after each step,
- putting the output together into a final result – determining a way of obtaining segmentation based on the outcome of quantum walks,
- assembling the above steps into a coherent algorithm.

These were the tasks that should have been completed in order to deliver the desired goal of this thesis.

3.3 Operator construction

Probably the most difficult task from the list above is construction of good evolution operators. These operators are the core of quantum walk, being responsible of how the walker explores the space and they obviously need to be dependent on the content of the image under segmentation.

Since every operator has to be unitary and the global phase is omittable (is not detectable when performing the measurement) the coin operator has to belong to special unitary group $SU(n)$:

Definition 10. *[50] **Special unitary group** of degree n, $SU(n)$, is a group of $n \times n$ unitary matrices, which determinants are equal to 1, with matrix multiplication as the group operation.*

$SU(1)$ is a degenerated group consisting of only one element - $\left[1\right]$, as there are no other 1×1 matrices satisfying the requirements.

Matrices from $SU(2)$ can be generally represented in the form of:

$$\begin{bmatrix} x & y \\ -\overline{y} & \overline{x} \end{bmatrix}, \quad |x|^2 + |y|^2 = 1, \tag{3.1}$$

where $x, y \in \mathbb{C}$ and $\overline{x}$ is a complex conjugate of x.

Another way to express this group is to decompose it according to Euler parametrization [51]:

$$\begin{gathered} SU(2) = e^{i\sigma_z\varphi} e^{i\sigma_y\theta} e^{i\sigma_z\psi} = \begin{bmatrix} \cos\theta e^{i(\psi+\varphi)} & \sin\theta e^{-i(\psi-\varphi)}) \\ -\sin\theta e^{i(\psi-\varphi)} & \cos\theta e^{-i(\psi+\varphi)} \end{bmatrix} \\ \theta \in [0, \frac{\pi}{2}], \quad \varphi \in [0, \pi], \quad \psi \in [0, 2\pi], \end{gathered} \tag{3.2}$$

where σ_y and σ_z are Pauli matrices. So, while constructing a 2×2 operator, one must specify 3 free parameters.

But from the perspective of two-dimensional walk the most interesting is the $SU(4)$ group, as the substantial part of coin operator, which modifies the coin state (C' in equation 2.11 and C_i in equation 2.12) is a 4×4 matrix. Basing on the above parametrization of $SU(2)$ there can

be performed Cartan decomposition of $SU(4)$ [52]:

$$SU(4) = SU(2) \otimes SU(2) e^{-i(\alpha_1 \sigma_x \otimes \sigma_x + \alpha_2 \sigma_y \otimes \sigma_y + \alpha_3 \sigma_z \otimes \sigma_z)} SU(2) \otimes SU(2), \tag{3.3}$$

where $\sigma_x, \sigma_y, \sigma_z$ are Pauli matrices and $\alpha_1, \alpha_2, \alpha_3 \in \mathbb{R}$.

The above equation indicates that there are as much as 15 degrees of freedom in $SU(4)$ decomposition. This means that it is not easy to find the right set of parameters to construct an appropriate operator. Among others, this will be the subject of the next chapter.

3.4 Summary

In this chapter was analyzed the problem formulated in the title of the thesis. There were recognized the main challenges that needed to be tackled in order to accomplish the appointed goal.

The questions and problems stated in this chapter would find a solution in the next one, 4, which presents the invented algorithms.

As was already shown in previous chapter, construction of quantum algorithms differs from design of the classical solutions, also the quantum walk model is not very similar to classical walks in terms of the structure. The most important and challenging task is finding appropriate evolution operators which determine the characteristics of the walk.

Chapter 4

Solution

This chapter addresses challenges discussed in the previous part of the document. Firstly, there are presented method for position space preparation and the general concept for tackling the problem stated in this thesis in sections 4.1 and 4.2, respectively. Then, there are proposed three solutions for performing image segmentation with quantum walks: one utilizing discrete-time quantum walks in section 4.3 and two using continuous-time model: one based on limiting distribution (section 4.4) and the other taking into account only the last state of the walk – section 4.5.

4.1 Position space preparation

Before proceeding to segmentation or even deciding on the quantum walk model, there occurs an initial task of loading an image and transforming it into a form that would be suitable for further processing.

In this thesis, there are considered two dimensional images which are expressed as matrices of pixels. Let the image be of size $M \times N$ (the number of rows and columns; respectively), then each pixel p_{ij} is described by two indices: $i \in \mathbb{Z}_M$ (index of the row) and $j \in \mathbb{Z}_N$ (index of the column). Each pixel can be represented as a single value of luminescence intensity or a vector of intensities in separate channels (e.g. vector of length 3 for the RGB color model).

Such image can be easily converted into a graph by taking each pixel as a vertex and

connecting it with its neighbors. The number of connections from a vertex to its neighbors determines the pool of possible moves. In this thesis, it is assumed that a walker can jump by distance of only one pixel either horizontally, or vertically. Therefore, each vertex of the graph is connected to 4 other (one to its left, right, above and below; except from the peripheral pixels, which have less connections) forming a regular grid.

In order to perform segmentation one needs to consider the similarities between adjacent pixels, as the more alike are the neighboring pixels, the greater is the chance that they belong to the same segment of the image. The constructed graph should take this into account and encourage the walker to head towards similar pixels and avoid crossing strong boundaries. This relationship can be expressed by putting a weight $w_{ij,kl}$ on each edge connecting any two pixels p_{ij} and p_{kl} of the graph. Here is applied the following formula proposed by Grady [1]:

$$w_{ij,kl} = \begin{cases} e^{-\frac{\beta d(p_{ij},p_{kl})}{\max d(p_{ij},p_{kl})}}, & \text{if } p_{ij} \text{ and } p_{kl} \text{ are connected,} \\ 0, & \text{otherwise,} \end{cases} \tag{4.1}$$

where $d(p_{ij}, p_{kl})$ is a metric of pixel similarity, defined below, and β is a free parameter that is responsible for highlighting the greater differences.

Definition 11. *In this work,* ***the metric*** $d(p_{ij}, p_{kl})$ ***for quantifying the similarity between two pixels*** p_{ij} ***and*** p_{kl}*, given in from of single values or vectors, is defined as follows:*

$$d(p_{ij}, p_{kl}) = \sum_c (p_{ij}[c] - p_{kl}[c])^2, \tag{4.2}$$

where c are the successive channels of pixels. The above expression is a square of the Euclidean distance, that has been chosen due to providing slightly better results than the standard Euclidean metric.

By defining weights of the graph with the formulas above, the more similar the neighboring pixels are, the greater the weight of the connection between them is. The next step is to design a quantum walker that is prone to advance over the edges with higher weight.

4.2 Concept outline

The main idea to tackle the problem of image segmentation with utilization of quantum walks is to start a separate walk for each seed and let the walker explore the image according to its content. Then, based on which walker was the most willing to explore given region of the image, divide it into segments.

As the input, the algorithm expects an image and a list of seeds – pixels with correct labels already assigned. The image is used to define a space of states for the walker as well as the evolution operators. After the construction of basic elements, a separate quantum walk is started from each provided seed. At the end of each step of a walk the probability distribution of measuring the walker at given position is recorded and upon finishing each walk the mean of the distributions is calculated. Finally, each pixel is assigned with label of the seed, for which walker starting from that seed expressed the highest limiting probability (see definition 7) of being measured at that pixel. Described process is illustrated in the figure 4.1.

Following sections present three detailed algorithms that fit into the above solution sketch:

- discrete time quantum walk solution (DTQW) – first attempt to perform the quantum walk based image segmentation which yielded promising results, but proved to be invalid due to some non-unitary transformations; nonetheless it was included in this document as a quantum walk inspired solution,
- continuous time quantum walk solution with limiting distribution(CTQW-LD) – this solution brings the most accurate results, but is a bit ineffective, especially if considered to be executed on a real quantum machine, as requires quantum state tomography (i.e. determining the exact quantum state) after each walker step,
- continuous time quantum walk solution - one shot (CTQW-OS) – this solution does not compute the limiting distribution but is interested only in the last state of the walker, therefore the quantum state needs to be reconstructed only once per walk (that is why it was named one shot), which significantly improves the algorithm performance, which is achieved for the price of a bit worse results in comparison to the other solutions.

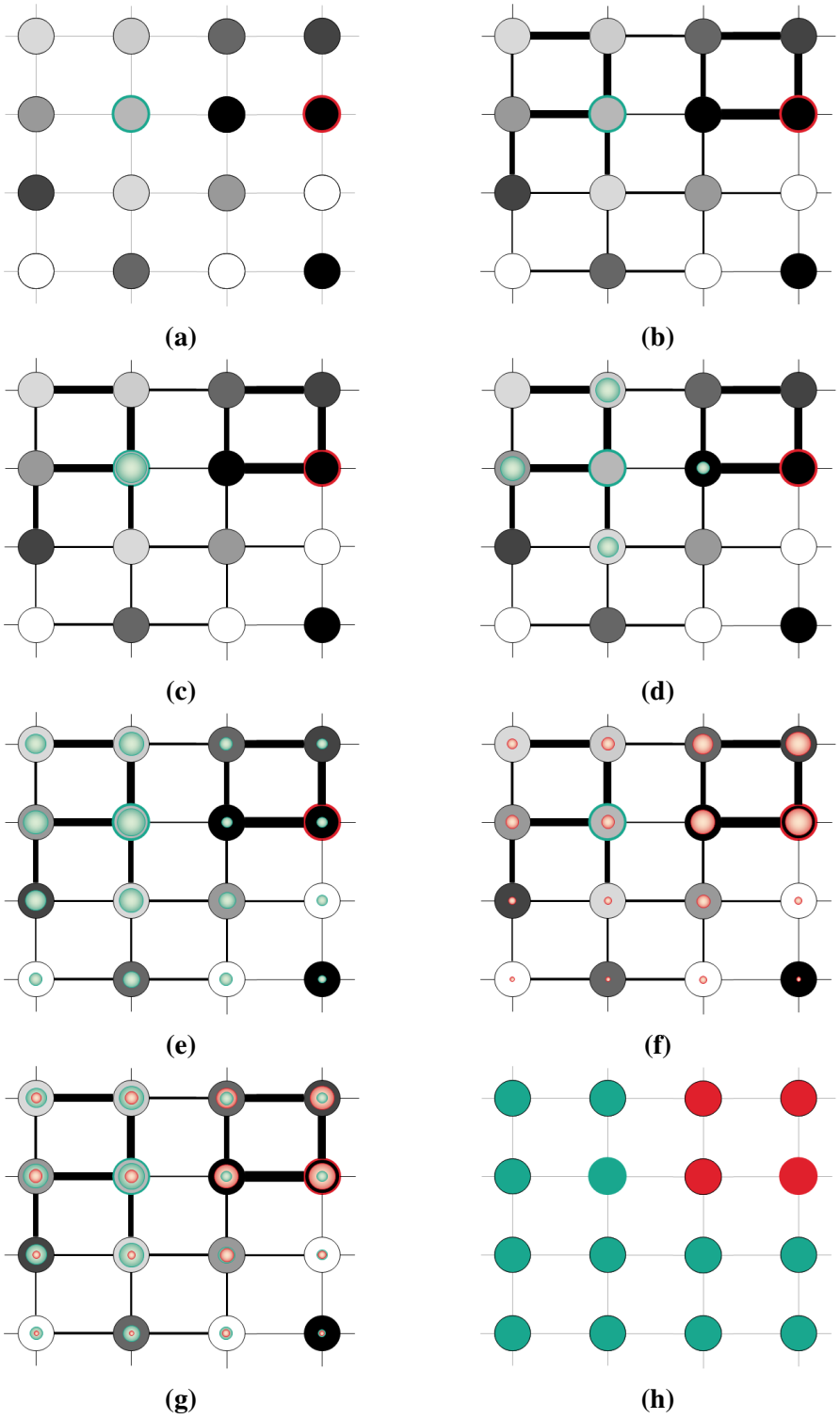

Figure 4.1: Visualization of the concept outline. 4.1a, as an input, the algorithm takes image (here big circles symbolize pixels with their intensity), as well as seeds (here two pixels with green and red ring). 4.1b, image is transformed into weighted graph based on intensities of neighboring pixels (weights are denoted by the edge width). 4.1c, a walk is started from a seed (colorful dots denote the probability of measuring walker at given pixel) and, 4.1d, proceeds for several steps. 4.1e, when the walk ends the limiting distribution is calculated. 4.1f, similar procedure is repeated for each walk. 4.1g, limiting distributions of each walk are compared and each pixel is assigned with label of the walk that had the highest mean probability of being measured at given pixel.

4.3 Solution 1.: Discrete time quantum walk (DTQW)

The first attempt was to utilize discrete time quantum walks. As described in the chapter 2.2, in order to perform this type of walk there need to be specified several elements: position and coin space, initial state of the walker, as well as shift and coin operators:

4.3.1 Position space

The position space defines the pool of possible locations for the walker. The input image has $N \times M$ pixels, all of which are admissible walker positions. The position space can be constructed by adding a separate basis state for each pixel and marking it with both its indices: $\{|00\rangle_p, |01\rangle_p, ..., |0(M-1)\rangle_p, |10\rangle_p, ..., |(N-1)0\rangle_p, |(N-1)1\rangle_p, ..., |(N-1)(M-1)\rangle_p\}$.

4.3.2 Coin space

The coin space is determined by the set of legal moves for the walker, which in two-dimensional case are: left, right, up and down. Then the basis of the coin space has the form: $\{|\leftarrow\rangle_c, |\rightarrow\rangle_c, |\uparrow\rangle_c, |\downarrow\rangle_c\}$.

4.3.3 Initial state

At the beginning the walker is located in one of the seeds of the image, hence the position space is initialized with a basis state corresponding to the seed. The coin state is an arbitrary basis state, e.g. left, $|\leftarrow\rangle_c$.

4.3.4 Shift operator

This operator is almost straightforwardly derived from its general form expressed by the equation 2.13. In the formula below the summation has to be rearranged in order to take into account the extreme cases of pixels on the frame of the image that do not have some of the

neighbors:

$$
\begin{aligned}
S = &\Big(\sum_{i=0}^{N-1}\sum_{j=1}^{M-1} |i(j-1)\rangle_p\langle ij|_p\Big)\otimes|\leftarrow\rangle_c\langle\leftarrow|_c + \\
&+\Big(\sum_{i=0}^{N-1}\sum_{j=0}^{M-2} |i(j+1)\rangle_p\langle ij|_p\Big)\otimes|\rightarrow\rangle_c\langle\rightarrow|_c + \\
&+\Big(\sum_{i=1}^{N-1}\sum_{j=0}^{M-1} |(i-1)j\rangle_p\langle ij|_p\Big)\otimes|\uparrow\rangle_c\langle\uparrow|_c + \\
&+\Big(\sum_{i=0}^{N-2}\sum_{j=0}^{M-1} |(i+1)j\rangle_p\langle ij|_p\Big)\otimes|\downarrow\rangle_c\langle\downarrow|_c.
\end{aligned}
\tag{4.3}
$$

4.3.5 Coin operator

Construction of coin operator is the most crucial task, as this operator determines the behavior of the walker. It is important that the walker explores the space by transition towards similar pixels rather than crossing sharp gaps between pixel values. This means that there is a need for harnessing inhomogeneous quantum walk, as the coin operator cannot be uniform, but should depend on the current walker position.

As it was shown in the previous chapter construction of 4×4 unitary operator requires specification of 15 parameters. Also, it is not obvious how each of them affects the final shape of the operator and the walk as the consequence. During studies concerning this model the author has not succeeded in finding any satisfying set of parameters. So, an alternative approach was needed.

The main difference between discrete time classical random walk and discrete time quantum random walk is the introduction of coin space in the latter case. The classical walker chooses its next state solely based on the current position, while its quantum counterpart, apart form the current position, keeps also knowledge of its orientation (as the coin space) which upon modification indicates the new state. In other words, the classical transition occurs in terms of change of position, while the quantum – in terms of alteration in direction (and only as a consequence the walker position changes). The quantum evolution operator effect is similar to telling the walker to turn by an arbitrary angle and then move straight ahead (exactly like it was in the Pearson model). This means that if quantum walker reaches the same pixel,

but from different directions the outcome of the coin operator (even thought at given position the operator is the same) could can be totally unlike. This makes the quantum walker behavior much more difficult to control.

The idea to address this issue relies on an attempt to make discrete time quantum walk a bit more similar to the classical case (i.e. eliminate the dependency to the walker orientation). Each vertex p_{ij} of the graph has four connections to its adjacent edges that have a weight which can be assigned to a variable (missing edges of extreme pixels have weight set to 0):

$$l_{ij} = w_{ij,i(j-1)}, \quad r_{ij} = w_{ij,i(j+1)}, \quad u_{ij} = w_{ij,(i-1)j}, \quad d_{ij} = w_{ij,(i+1)j} \tag{4.4}$$

and normalized in order to make their squares add up to 1:

$$\begin{aligned} \overline{l_{ij}} &= \sqrt{\frac{l_{ij}}{l_{ij}+r_{ij}+u_{ij}+d_{ij}}}, \quad \overline{r_{ij}} = \sqrt{\frac{r_{ij}}{l_{ij}+r_{ij}+u_{ij}+d_{ij}}}, \\ \overline{u_{ij}} &= \sqrt{\frac{u_{ij}}{l_{ij}+r_{ij}+u_{ij}+d_{ij}}}, \quad \overline{d_{ij}} = \sqrt{\frac{d_{ij}}{l_{ij}+r_{ij}+u_i+d_i}}. \end{aligned} \tag{4.5}$$

The desired coin state after applying coin operator at pixel p_{ij} would look more less like that:

$$|c_{ij}\rangle_c = \overline{l_{ij}}|\leftarrow\rangle_c + \overline{r_{ij}}|\rightarrow\rangle_c + \overline{u_{ij}}|\uparrow\rangle_c + \overline{d_{ij}}|\downarrow\rangle_c. \tag{4.6}$$

The idea was to construct the following coin operator:

$$C = \sum_{i,j} (|ij\rangle_p\langle ij|_p \otimes (|c_{ij}\rangle_c\langle\leftarrow|_c + |c_{ij}\rangle_c\langle\rightarrow|_c + |c_{ij}\rangle_c\langle\uparrow|_c + |c_{ij}\rangle_c\langle\downarrow|_c)). \tag{4.7}$$

This operator applied to an arbitrary state $|\phi\rangle = |ij\rangle_p \otimes (x|\leftarrow\rangle_c + y|\rightarrow\rangle_c + z|\uparrow\rangle_c + w|\downarrow\rangle_c)$ yields the following state:

$$\begin{aligned} |\phi'\rangle = C|\phi\rangle &= |ij\rangle_p \otimes (\overline{l_{ij}}(x+y+z+w)|\leftarrow\rangle_c + \overline{r_{ij}}(x+y+z+w)|\rightarrow\rangle_c \\ &\quad + \overline{u_{ij}}(x+y+z+w)|\uparrow\rangle_c + \overline{d_{ij}}(x+y+z+w)|\downarrow\rangle_c) \\ &= |ij\rangle_p \otimes ((x+y+z+w)|c_{ij}\rangle_c). \end{aligned} \tag{4.8}$$

Unfortunately, the effect is not exactly correct from the quantum computation point of view, as it is the sum of squares of coefficients: $x^2 + y^2 + z^2 + w^2$ that equals 1, not the $x + y + z + w$. So, the norm of the walker state is not preserved. This means, that the proposed coin operator C is not unitary and therefore cannot be utilized in a quantum algorithm.

Nevertheless, it provides quite reasonable results (they are presented in the chapter 5) and can be regarded as a classical quantum-inspired solution for image segmentation.

4.3.6 Algorithm

Algorithm 1 presents a step by step procedure for performing the image segmentation with the constructed DTQW solution:

Algorithm 1: Image segmentation using discrete time quantum walk solution (DTQW)

Input: Image $A = (a_{ij}) \in V^{M \times N}$, where $V = \mathbb{R}^c$ and c is number channels for a pixel,
Set of labels L,
List of seeds $S = \{(p_1, l_1), ..., (p_n, l_n)\}$, where $p_k \in \mathbb{Z}_M \times \mathbb{Z}_N$ is the seed position and $l_k \in L$ is its label.

Parameters : β - boundary strengthening parameter,
T - number of steps of the walk.

Output: Segmented image $B = (b_{ij}) \in L^{M \times N}$.

$W \leftarrow calculate\_weights(A, \beta)$; // according to the formula 4.1
$S \leftarrow construct\_shift\_operator(A)$; // based on the equation 4.3
$C \leftarrow construct\_coin\_operator(W)$; // folowing the formula 4.7
$U \leftarrow SC$
foreach $(q_k, l_k) \in S$ **do** // perform walk for each seed
  $|\psi_0\rangle_p \leftarrow |q_k\rangle_p$; // set initial state to the seed
  for $t \leftarrow 1$ **to** T **do**
    $|\psi_t\rangle_p \leftarrow U|\psi_{t-1}\rangle_p$; // perform a move
    $\vec{D}_t \leftarrow retrive\_position(|\psi_t\rangle_p)$; // prob. dist. of measuring walker at each position
  end
  $L\vec{D}_k \leftarrow \frac{1}{T}\sum_{t=1}^{T} \vec{D}_t$; // limiting distribution of the walk
end
for $i \leftarrow 0$ **to** $M-1$ **do**
  for $j \leftarrow 0$ **to** $N-1$ **do**
    $k \leftarrow find\_seed(LD, i, j)$; // find seed that on average has the highest probability of being measured at pixel ij
    $B_{ij} \leftarrow l_k$; // assign label to the pixel
  end
end

4.4 Solution 2.: Continuous time quantum walk with limiting distribution (CTQW-LD)

An alternative way to perform the task is to utilize the continuous time quantum walk model. As opposed to the former solution there is only one space and one evolution operator among elements that need to be specified in order to perform this kind of walk.

4.4.1 Position space

The position space remains the same as in the discrete time quantum walk: $\{|00\rangle_p, |01\rangle_p, ..., |0(M-1)\rangle_p, |10\rangle_p, ..., |(N-1)0\rangle_p, |(N-1)1\rangle_p, ..., |(N-1)(M-1)\rangle_p\}$.

4.4.2 Initial state

The initial state has now a simpler form as there is only one subsystem to initialize - the position is set to a basis state corresponding to one of the given seeds.

4.4.3 Evolution operator

According to the discussion in the previous chapter, the general form of the evolution operator in continuous time quantum walk is as follows (here i means imaginary unit):

$$U(t) = e^{-iHt}. \tag{4.9}$$

The task is to find an appropriate Hamiltonian matrix H. It has to be a square matrix of size $MN \times MN$ that would be hermitian (this ensures that the operator $U(t)$ is unitary, as has been proved in the lemma 2). It also has to yield satisfying results in terms of position space exploration by the walker according to the content of the image.

The idea is to construct the Hamiltonian based on the weights matrix defined by the equation 4.1 and a free real parameter γ that determines the rate of spread of the quantum

walk:

$$H_{ij,kl} = \begin{cases} -\gamma w_{ij,kl}, & \text{if } i \neq k \vee j \neq l. \\ \gamma \sum_{k',l'} w_{ij,k'l'}, & \text{if } i = k \wedge j = l. \end{cases} \tag{4.10}$$

Please notice, that since weight matrix is symmetrical ($w_{ij,kl} = w_{kl,ij}$) and its values are real numbers, the constructed matrix H is a hermitian matrix and therefore the operator $U(t)$ is unitary.

4.4.4 Algorithm

Algorithm 2 presents a step by step procedure for performing the image segmentation with the constructed CTQW-LD solution:

Algorithm 2: Image segmentation using continuous time quantum walk with limiting distribution solution (CTQW-LD)

Input: Image $A = (a_{ij}) \in V^{M \times N}$, where $V = \mathbb{R}^c$ and c is number channels for a pixel,
Set of labels L,
List of seeds $S = \{(p_1, l_1), ..., (p_n, l_n)\}$, where $p_k \in \mathbb{Z}_M \times \mathbb{Z}_N$ is the seed position and $l_k \in L$ is its label.

Parameters : β - boundary strengthening parameter,
γ - rate of spread of the walker,
T - number of steps of the walk.

Output: Segmented image $B = (b_{ij}) \in L^{M \times N}$.

$W \leftarrow calculate\_weights(A, \beta)$; // according to the formula 4.1
$H \leftarrow construct\_hamiltonian(W, \gamma)$; // based on the equation 4.10
$U \leftarrow construct\_operator(H)$; // $U = U(1) = e^{-iH}$
foreach $(q_k, l_k) \in S$ **do** // perform walk for each seed
  $|\psi(0)\rangle_p \leftarrow |q_k\rangle_p$; // set initial state to the seed
  for $t \leftarrow 1$ **to** T **do**
    $|\psi(t)\rangle_p \leftarrow U|\psi(t-1)\rangle_p$; // perform a move
    $\vec{D}_t \leftarrow retrive\_position(|\psi(t)\rangle_p)$; // prob. dist. of measuring walker at each position
  end
  $L\vec{D}_k \leftarrow \frac{1}{T}\sum_{t=1}^{T} \vec{D}_t$; // limiting distribution of the walk
end
for $i \leftarrow 0$ **to** $M-1$ **do**
  for $j \leftarrow 0$ **to** $N-1$ **do**
    $k \leftarrow find\_seed(LD, i, j)$; // find seed that on average has the highest probability of being measured at pixel ij
    $B_{ij} \leftarrow l_k$; // assign label to the pixel
  end
end

4.5 Solution 3.: Continuous time quantum walk - one shot (CTQW-OS)

During work on the above algorithm it turned out that it would be interesting to consider yet another approach. This solution is almost identical to the CTQW-LD, but instead of calculating the limiting distribution of each walk, only the distribution after last state is used. As it will be shown in the next chapter, this method gives results with a bit worse segmentation accuracy, but for careful choice of parameters the difference is ommitable. However, it does not require obtaining the probability distribution after each step, which is a tremendous profit, especially if the algorithm would be executed on a real quantum device, where the quantum state cannot be obtained directly, but needs to be recreated by multiple repetition of experiment ended with a measurement.

4.5.1 Algorithm

Algorithm 3 presents a step by step procedure for performing the image segmentation with the constructed CTQW-OS solution:

Algorithm 3: Image segmentation using continuous time quantum walk – one shot solution (CTQW-OS)

Input: Image $A = (a_{ij}) \in V^{M \times N}$, where $V = \mathbb{R}^c$ and c is number channels for a pixel,
Set of labels L,
List of seeds $S = \{(p_1, l_1), ..., (p_n, l_n)\}$, where $p_k \in \mathbb{Z}_M \times \mathbb{Z}_N$ is the seed position and $l_k \in L$ is its label.

Parameters : β - boundary strengthening parameter,
γ - rate of spread of the walker,
T - number of steps of the walk.

Output: Segmented image $B = (b_{ij}) \in L^{M \times N}$.

$W \leftarrow calculate\_weights(A, \beta)$; // according to the formula 4.1
$H \leftarrow construct\_hamiltonian(W, \gamma)$; // based on the equation 4.10
$U \leftarrow construct\_operator(H)$; // $U = U(1) = e^{-iH}$
foreach $(q_k, l_k) \in S$ **do** // perform walk for each seed
  $|\psi(0)\rangle_p \leftarrow |q_k\rangle_p$; // set initial state to the seed
  for $t \leftarrow 1$ **to** T **do**
    $|\psi(t)\rangle_p \leftarrow U|\psi(t-1)\rangle_p$; // perform a move
  end
  $\vec{D}_k \leftarrow retrive\_position(|\psi(T)\rangle_p)$; // prob. dist. of measuring walker at each position after last step
end
for $i \leftarrow 0$ **to** $M-1$ **do**
  for $j \leftarrow 0$ **to** $N-1$ **do**
    $k \leftarrow find\_seed(D, i, j)$; // find seed that has the highest probability of being measured at the end of the walk at pixel ij
    $B_{ij} \leftarrow l_k$; // assign label to the pixel
  end
end

4.6 Summary

In this chapter there were proposed three methods for performing image segmentation with quantum walks. The first one, based on discrete time quantum walks (DTQW), turned out to be not completely compliant with the rules of quantum computing, as the evolution operator is not unitary. Nevertheless, it was included in this thesis as a quantum walk based solution, due to its quite good results. The remaining solutions utilize continuous time quantum walks. CTQW-LD, calculates limiting distribution of quantum walks and provides the most accurate results, but is not very effective especially in perspective of executing this algorithm on a quantum computer. CTQW-OS, does not require obtaining the limiting distribution, but focuses only on the final state of the walk. Therefore it is much more efficient, and its results are not much worse than CTQW-LD, as it will be shown in the next chapter.

The elaborated solutions, as every other algorithm, required testing and evaluation. Results of this analysis are presented in the following chapter, 5.

Chapter 5

Evaluation

This chapter analyzes the solutions formulated in the previous chapter 4 in terms of the resulting segmentation accuracy (section 5.1 describes scenarios, while section 5.2 presents results of performed tests) as well as the performance of simulations of proposed algorithms, in section 5.3.

5.1 Experiments description

In order to evaluate the quality of proposed solutions there had to be performed some tests of accuracy of obtained segmentation.

5.1.1 Dataset

As the source for test images the Berkeley Segmentation Dataset and Benchmark, BSDS500 [53], was used. This dataset contains a multitude of photographs, both in color and in grayscale. Each of them has several contour images performed manually by people. The outlines differ by number of distinguished segments and by a level of details. The image segmentation is quite subjective task, especially when the borders in the picture are blurred and unclear, the same image can be segmented quite differently by various people.

For testing purposes there have been chosen a few samples from BSDS500 dataset - three RGB and three grayscale picture. For each of them there was also taken one outline image

which served as a reference.

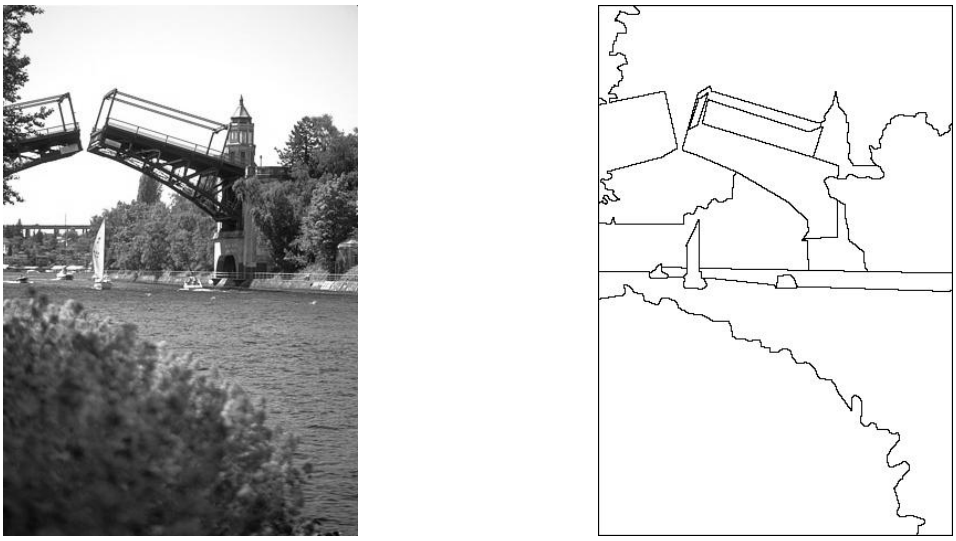

(a) original photograph **(b)** outline image prepared manually by a human

Figure 5.1: A sample from the Berkeley Segmentation Dataset and Benchmark, BSDS500 [53].

5.1.2 Parameters

The most important parameter for the proposed solution is the set of seeds. Seeds need to be provided separately and the algorithm does not specify a way to obtain them. Here, for each sample image there are prepared four sets of seeds:

- One set is chosen manually by the author of this thesis. In order to archive better results the seeds are spread quite uniformly over the image, avoiding introducing areas of high density of seeds of one class in the close proximity of seedless areas. Also a bit higher concentration of seeds is kept around borders, especially the weak and unclear boundaries. The set contains about 0.2% pixels of the whole image.
- The other three sets are prepared automatically by drawing uniformly a fraction of pixels from the image and assigning them with the labels based on the ground truth segmentation from BSDS500 dataset. The fraction of pixels drown for the second, third and fourth set of seeds is 0.2%, 0.5% and 1%, respectively.

Additionally, there are also three free parameters, that need to be taken into consideration and have the optimal value estimated:

- β – it is used during weights calculation. The greater its value, the more significant are the stronger differences between pixels. So the high β parameter makes the walker stay closer to it seed rather than disperse and explore further regions.

- T – determines the number of steps (number of applications of the evolution operator) before the walk stops. It has a great impact on the final outcome. If the T value is too small then some walker might have no chance to explore sufficiently the image, which can result in some parts of the segment that should belong to this walker, being annexed by a walker from a different segment, that for example, started from the closer seed and managed to overstep the boundaries. It can also cause appearance of some blank areas that have not been covered by any of the walkers. On the other hand, if parameter T is too high, then the walk might proceed long enough that the walkers diffusion to neighboring segments causing the segmentation quality worsen over time.

- γ – this parameter is only used in solutions based on continuous time quantum walks. It determines the rate of spread of the walker. So, the greater the value of this parameter, the greater is the area explored by the walker upon a single application of evolution operator. This means one could set γ to a high value to limit the number of steps. But this would result in the decreased sensitivity of the segmentation to details and would hugely smoothen and oversimplify the boundaries of resulting segments. So, the value of this parameter should be small in order to gain higher precision.

5.1.3 Scenario

Apart from the three invented solutions, there was also implemented the Grady's algorithm for image segmentation utilizing classical random walks [1]. It served as a point of reference additional to the ground truth segmentation obtained from the manually created image outlines included in BSDS500 dataset.

Next, all four methods (three proposed algorithm and the Grady's method) with different combinations of the parameters were used to perform segmentation of test images. Each

segmentation was then compared against the ground truth images and finally there was calculated the percentage of pixels with consentaneous labels.

5.1.4 Experiments infrastructure

The test of the proposed solutions could not obviously be performed on the real quantum device, as the requirements for the algorithm (for example the number of qubits needed to express the walker state, and the level of customization the quantum operators, that need to be tailor-made for each processed images) are beyond the capabilities of currently accessible quantum computers, like IBM-Q [54] or Rigetti [55]. Therefore, there had to be performed a simulation of quantum computations on a classical machine.

The project code has been prepared using Python language (version 3.4.3) with *QuTiP* software (version 4.2.0), a very convenient open-source Python library for simulation of quantum systems, that under the hood highly utilizes matrix algebra. The program was executed on a computer with processor Intel® Core™ i5-4210M and 16GB of RAM.

5.2 Results

5.2.1 Configuration adjustment

At first there was analyzed impact of the parameters on the accuracy of segmentation. After choice of the ranges of parameters β, γ, T, there have been performed multiple segmentations with different configurations. Each set of parameters was used to obtain segmentation of every test image with different sets of seeds. The results have been compared against the reference segmentation from BSDS500 dataset. Average scores have been visualized on the heatmaps, which allowed to estimate optimal configurations:

- DTQW solution (figure 5.2): $(\beta = 90.0, T = 60)$,
- CTQW-LD solution (figure 5.3): $(\beta = 150.0, \gamma = 0.001, T = 20000)$,
- CTQW-OS solution (figure 5.4): $(\beta = 150.0, \gamma = 0.001, T = 5000)$.

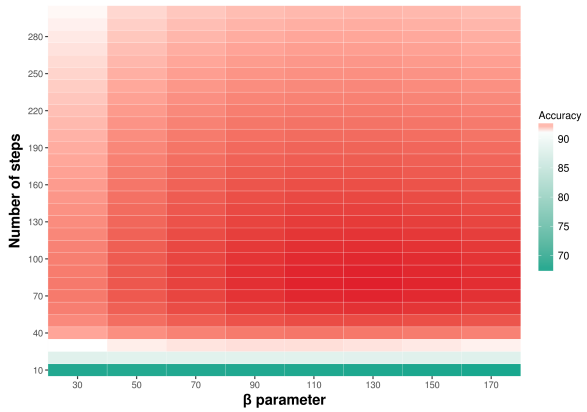

Figure 5.2: Average segmentation accuracy (over various test images and different set of seeds) of the discrete time quantum walk (DTQW) algorithm in reference to the manual segmentation from BDSD500 dataset, depending on the values of β and T parameters. The heatmap indicates that within those ranges for parameters the best results of the DTQW might be obtained for configuration: $\beta = 90.0, T = 60$, or a similar one.

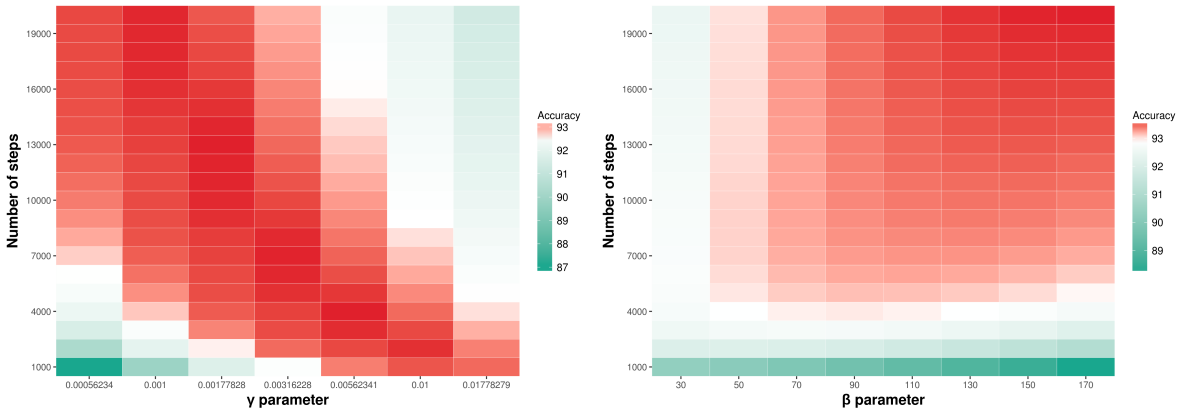

(a) **(b)**

Figure 5.3: Average segmentation accuracy (over various test images and different set of seeds) of the continuous time quantum walk with limiting distribution (CTQW-LD) algorithm in reference to the manual segmentation from BDSD500 dataset, depending on the chosen configuration: chart 5.3a influence of γ and T parameters for a fixed value of $\beta = 90.0$; chart 5.3b influence of β and T parameters for a fixed value of $\gamma = 0.001$. The heatmaps indicate that within those ranges for parameters the best results of the CTQW-LD might be obtained for configuration: $\beta = 150.0, \gamma = 0.001, T = 20000$, or a similar one.

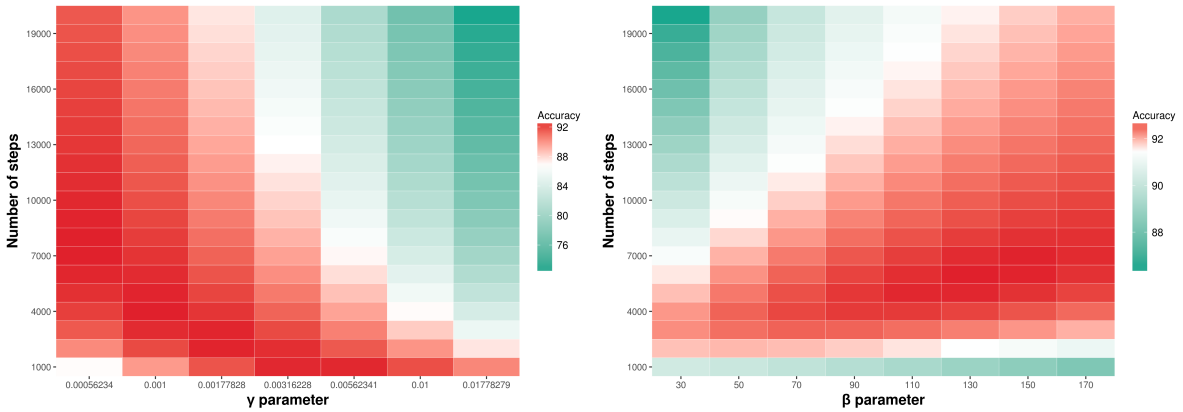

(a) **(b)**

Figure 5.4: Average segmentation accuracy (over various test images and different set of seeds) of the continuous time quantum walk one shot (CTQW-OS) algorithm in reference to the manual segmentation from BDSD500 dataset, depending on the chosen configuration: chart 5.4a influence of γ and T parameters for a fixed value of $\beta = 90.0$; chart 5.4b influence of β and $steps$ parameters for a fixed value of $\gamma = 0.001$. The heatmaps indicate that within those ranges for parameters the best results of the CTQW-OS might be obtained for configuration: $\beta = 150.0, \gamma = 0.001, T = 5000$, or a similar one.

5.2.2 Accuracy evaluation

Figure 5.5 shows segmentations of two sample images: a seashore landscape in color in 5.5a and a man under a tree in grayscale in 5.5h. Then there are reference segmentations: 5.5b and 5.5i are ground truth images included in BSDS500 dataset, while 5.5d and 5.5k were prepared using Grady's algorithm. The last three images for each photo were obtained with algorithms proposed in this thesis: 5.5e and 5.5l present results of DTQW solution, 5.5f and 5.5m come from CTQW-LD algorithm, while 5.5g and 5.5n – CTQW-OS method. DTQW algorithm seems to give the worst effects, as the formed segments are often shapeless. As could be expected CTQW-OS is a bit inferior to CTQW-LD. Nevertheless the difference is not obvious, thanks to careful choice of parameters (especially number of steps), while the gain in terms of performance is tremendous. CTQW-LD looks comparably, if not better (please notice the head of the man under tree) than Grady's method. Of course, all of these solutions are imperfect which can be clearly seen in the areas of weak and unobvious margins (like, the

line of horizon or leaves of the tree).

	manual seeds 0.2%	automatic seeds 0.2%	automatic seeds 0.5%	automatic seeds 1.0%
Grady ($\beta = 90.0$)	93.50	90.25	93.50	94.88
Grady ($\beta = 150.0$)	93.63	90.38	93.50	94.88
DTQW ($\beta = 90.0, T = 100$)	90.58	89.03	92.96	94.47
DTQW ($\beta = 150.0, T = 100$)	90.16	88.90	93.06	94.55
CTQW-LD ($\beta = 150.0, \gamma = 0.001, T = 20000$)	93.40	90.89	93.48	94.72
CTQW-LD ($\beta = 90.0, \gamma = 0.0032, T = 10000$)	93.33	90.99	93.12	94.22
CTQW-OS ($\beta = 150.0, \gamma = 0.001, T = 5000$)	88.60	88.84	92.92	94.26
CTQW-OS ($\beta = 150.0, \gamma = 0.001, T = 10000$)	90.86	89.56	92.07	92.92

Table 5.1: Average accuracy (over test images) of developed algorithms as well as Grady's method for different sets of seeds.

Table 5.1 presents average accuracy (over test images) of developed algorithms in comparison to Grady's method for different sets of seeds. It clearly shows that the segmentation accuracy increases with the size of seeds set. Manually chosen seeds give better results than the same amount of automatically drawn ones, due to careful selection. The most accurate of the proposed solutions is CTQW-LD algorithm, which gives almost as good results as reference algorithm or even excels it in some cases. The other methods express slightly worse performance. The last two rows show how sensitive to the walk duration is the CTQW-OS solution; the accuracy drops significantly if the number of steps is too high.

However, for optimal configuration of parameters all developed methods give decent results. The only unfavorable aspect is the quite considerable amount of seeds needed to obtain satisfactory segmentation accuracy. As the 0.2% seems to be a bit too little, there has to be specified about 0.5% seeds, which for image of size 320x480 means that over seven hundred of pixels need to be labeled.

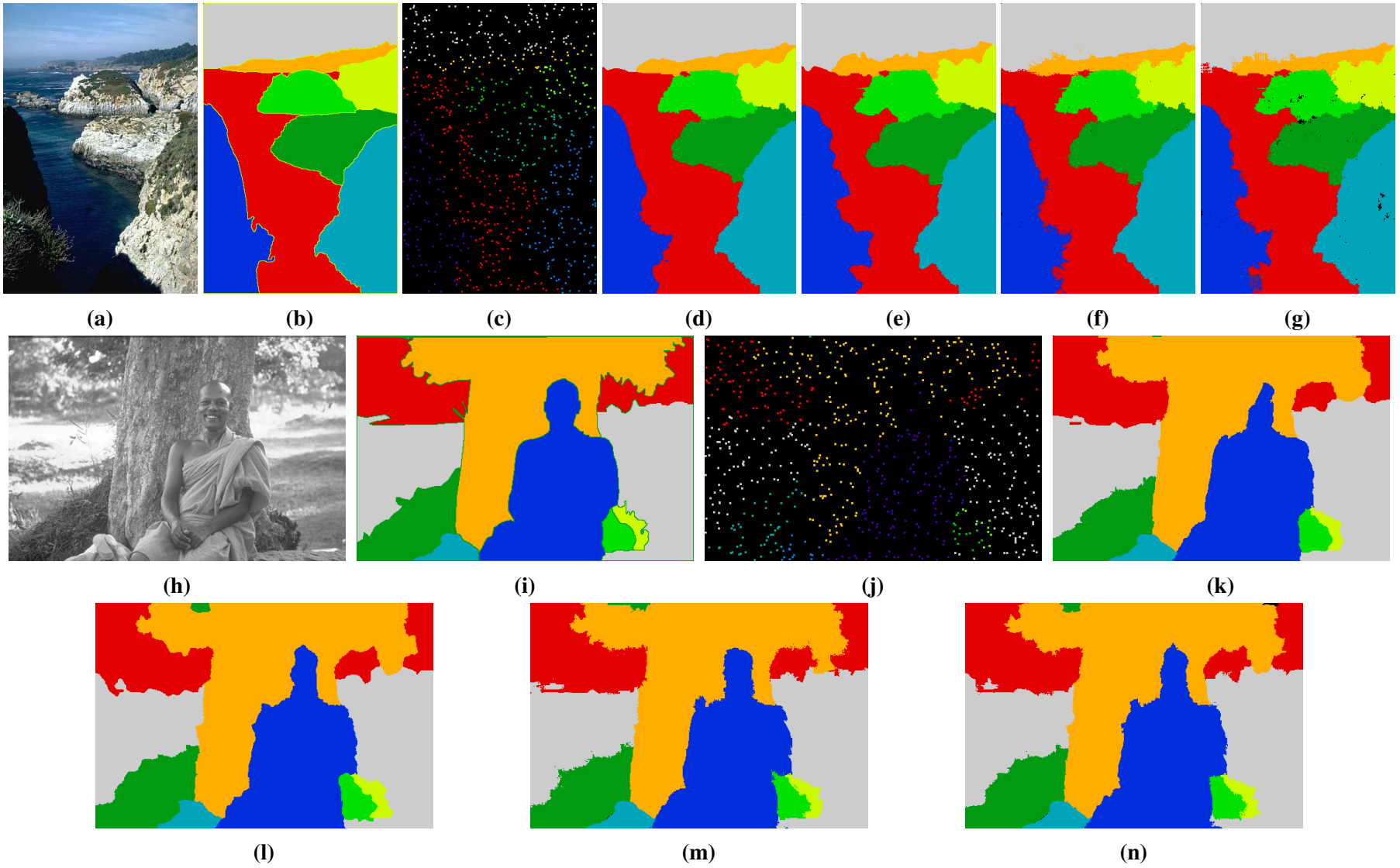

Figure 5.5: Summary of obtained results on an example of two test images one in color, the other in grayscale. First two pictures come directly from the BSDS500 dataset: the original image (5.5a, 5.5h) and the manual segmentation (5.5b, 5.5i). The black dotted images (5.5c, 5.5j) present input seeds for the segmentation, which constitute 0.5% of all pixels in the image. Then there is included the other reference segmentation obtained with Grady's algorithm(5.5d, 5.5k). Finally, the last three images present the results of proposed algorithms: DTQW(5.5e, 5.5l), CTQW-LD(5.5f, 5.5m) and CTQW-OS(5.5g, 5.5n) for the optimal configuration specified in the previous subsection.

5.3 Performance evaluation

5.3.1 Optimization methods

In the course of simulations, there have been introduced some technical improvements, that did not influence the resulting segmentation, but significantly enhanced the performance, allowing to accelerate the program execution. The gain in comparison to the first, quite naive approach, was on the level of three, or even four orders of magnitude:

- It has been noticed, that the walks starting from seeds with the same label can be assembled into one walk with the initial state as the superposition of the basis states corresponding to those seeds. In this way, the number of walks performed in a single segmentation task has been reduced from hundreds or even thousands to about a dozen (specifically the number of different labels).

- Since each walk is totally independent from the others they can be performed in parallel in separate processes. This allowed for full exploitation of every core of the processor.

- To quite accurately estimate the limiting distribution of a walk (in the case of CTQW-LD method) it is sufficient to calculate the mean distribution after every few steps. It was tested that taking into account distributions after only about 1% of steps quite uniformly sampled from the range $[1, T]$ gives almost undisturbed results. In order to exploit this observation, the simulation of the walk was altered – instead of performing each step in a loop by repeated application of the evolution operator U to the current state, there was used *mesolve* function from *QuTiP* library, that takes the Hamiltonian H, the list of time points at which the quantum system state will be obtained, and performs master equation evolution, by solving a system of differential equations to calculate only the desired states. This allows to avoid the time-consuming iterative application of operator U for thousands of times.

5.3.2 Performance results

As in case of the segmentation accuracy, also the execution time of proposed methods is highly dependent on the chosen configuration. Each walk runs for a given number of steps, so the program duration increases with the parameter T. Also the value of γ is significant, as the higher values of the parameter densify the walker state early in the course of walk, which affects the time of matrix multiplication. For comparison, the Grady's classical algorithm is quite time efficient, as utilizes an asymptotic approach and has only one free parameter, β, which is irrelevant in terms of performance, so its duration is constant for images of given size.

Before optimization a segmentation of a single image would take several hours. Upon introduction the aforementioned enhancements the performance of the solutions was boosted so much, that for certain configurations the execution time of the simulation for the images from BSDS500 dataset is of the same order of magnitude as the reference algorithm, while still providing results with similar accuracy.

The average execution times for test images of size 320x480 and optimal configurations specified in section 5.2 were as follows: about 30 seconds for DTQW solution, 5-6 minutes for CTQW-LD and around a minute in case of CTQW-OS method. Along with the growth of γ or T the duration of the calculations increases linearly. For comparison Grady algorithm for the same samples requires about 30 seconds.

This means that developed solutions are comparable both in terms of accuracy as well as performance to Grady algorithm. Of course, these are the execution times of simulation on classical computer which would not practically matter during transition to a quantum device, nevertheless the proposed results, especially CTQW-OS, are expected to do well also in quantum conditions.

5.4 Quantum realization possibilities

A crucial difference between simulation and the actual execution of the algorithm on a quantum computer is the fact, that during simulation, there is always access to the whole quantum state. In real conditions the actual state of the particle is not known until measurement, which reduces it to one of the basis states according to probability distribution determined by the

current state. So, to gain the knowledge on the walker state after a given number of steps, one needs to perform the same walk multiple times and measure it in order to reconstruct the probability distribution.

In these conditions the CTQW-LD solution is not very effective in quantum case – in order to obtain the limiting distribution the experiment has to be repeated several times for different numbers of steps. For this reason, it would be vastly beneficial to apply the CTQW-OS algorithm, which requires requires the construction of the probability distribution only once per walk.

5.5 Summary

This chapter presented results of elaborated methods, which show that proposed algorithms induce quite decent segmentation, that is of similar accuracy to the reference method invented by Grady [1]. There was analyzed the influence of parameters on the outcome segmentation as well as the performance of presented solutions, and ultimately the optimal configurations were found. There were also proposed some optimization methods to the invented algorithms, which without changing the underlying mechanisms of proposed concepts allowed for a huge performance boost during simulations of the algorithms.

Chapter 6

Conclusion

This chapter summarizes the efforts put in this thesis as well as obtained results. Section 6.1 examines accomplishment of the goals specified in the Introduction, while section 6.2 indicates directions in which work in this field might proceed.

6.1 Achieved goals

At the end of the work on this thesis comes time to revise what has managed to be achieved. The goals of the thesis, specified in the section 1.3 have been successfully completed:

Research in the field of quantum walks

There were conducted exhaustive studies concerning quantum computation and quantum walks as well as matrix algebra and image segmentation. As the result of this research there emerged the second chapter, 2, of this thesis, which treats about the theoretical background of the quantum walks.

Quantum walk model development

There have been analyzed the applicability of two types of quantum walks: discrete time and continuous time quantum walks. Both of those models served as base for developed solutions.

The discrete time solution turn out to be imperfect, but the continuous time walks can be successfully harnessed to perform image segmentation with quantum walks.

Elaboration of an algorithm

Three image segmentation algorithms constitute the main contribution of this work:

- discrete time solution (DTQW) – this method based on an attempt of a straightforward translation of classical random walks to the quantum world. Unfortunately, the proposed coin operator is not unitary, therefore this solution cannot be utilized on a quantum computer.
- continuous time solution with limiting distribution (CTQW-LD) – the segmentation is obtained based on the mean probability distribution of measuring the walker at every position after each step. It gives the finest results, but requires the quantum state tomography after every step of the walk. On quantum devices this is an expensive operation, therefore this solution would be quite inefficient.
- continuous time one shot solution (CTQW-OS) – instead of calculating the limiting distribution, only the last state of the walk is required. Compared to the previous solution, this saves on the quantum state tomography, which needs to be performed only once, while the resulting segmentation is not much worse than in CTQW-LD case.

Implementation and simulation of the algorithm

The invented algorithms have been implemented in Python language and simulated on classical computer. The results turned out to be on the similar level as the reference Grady's algorithm utilizing classical random walks – above 90% percents of accuracy compared to the ground truth segmentation prepared manually.

6.2 Future works

The segmentation utilized in this work is a seeded-based method. User has to specify, apart from the image, a set of pixels with assigned segment to which they belong. This means that it is not totally automatic approach. Also to achieve good results a considerable amount of seeds needs to be provided. This is a field for improvement; either a way to limit the number of required seeds or a method for automatic specifying the seeds would significantly increase the user experience while using the proposed solutions for image segmentation.

The other possible direction for future development in the topic of images segmentation with quantum walks would be improvement of the DTQW solution. Presented method gives good results, but the chosen operator does not adhere to rules of quantum computation. If one would propose a better operator this could result in quite reasonable solution. In the section 3.3, there was shown that coin operator can be described by 15 parameters, which is the biggest obstacle, as it is not clear how each of the parameters affects the walk.

Appendix A

Publication

Based on the results obtained in this thesis there is being prepared a paper presenting developed solutions:

> Michał Krok, Katarzyna Rycerz, Piotr Gawron: Application of continuous time quantum walks to image segmentation, *in preparation*.

List of Tables

List of Figures

Bibliography

[1] Leo Grady. Random walks for image segmentation. *IEEE Transactions on Pattern Analysis and Machine Intelligence*, 28(11):1768–1783, 2006.

[2] Richard P. Feynman. Plenty of Room at the Bottom. *American Physical Society*, (December):1–11, 1959.

[3] Noah Linden, Hervé Barjat, and Ray Freeman. An implementation of the Deutsch-Jozsa algorithm on a three-qubit NMR quantum computer. *Chemical Physics Letters*, 296(October):61–67, 1998.

[4] L. Dicarlo, J. M. Chow, J. M. Gambetta, Lev S. Bishop, B. R. Johnson, D. I. Schuster, J. Majer, A. Blais, L. Frunzio, S. M. Girvin, and R. J. Schoelkopf. Demonstration of two-qubit algorithms with a superconducting quantum processor. *Nature*, 460(7252):240–244, 2009.

[5] Fazhan Shi, Xing Rong, Nanyang Xu, Ya Wang, Jie Wu, Bo Chong, Xinhua Peng, Juliane Kniepert, Rolf Simon Schoenfeld, Wolfgang Harneit, Mang Feng, and Jiangfeng Du. Room-temperature implementation of the deutsch-jozsa algorithm with a single electronic spin in diamond. *Physical Review Letters*, 105(4):2–5, 2010.

[6] R. Harris, M. W. Johnson, T. Lanting, A. J. Berkley, J. Johansson, P. Bunyk, E. Tolkacheva, E. Ladizinsky, N. Ladizinsky, T. Oh, F. Cioata, I. Perminov, P. Spear, C. Enderud, C. Rich, S. Uchaikin, M. C. Thom, E. M. Chapple, J. Wang, B. Wilson, M. H. S. Amin, N. Dickson, K. Karimi, B. Macready, C. J. S. Truncik, and

G. Rose. Experimental Investigation of an Eight Qubit Unit Cell in a Superconducting Optimization Processor. 2010.

[7] R Barends. Digitized Adiabatic Quantum Computing with a Superconducting Circuit. *arXiv*, page 1511.03316, 2015.

[8] S. Debnath, N. M. Linke, C. Figgatt, K. A. Landsman, K. Wright, and C. Monroe. Demonstration of a small programmable quantum computer with atomic qubits. *Nature*, 536(7614):63–66, 2016.

[9] T. F. Watson, S. G.J. Philips, E. Kawakami, D. R. Ward, P. Scarlino, M. Veldhorst, D. E. Savage, M. G. Lagally, Mark Friesen, S. N. Coppersmith, M. A. Eriksson, and L. M.K. Vandersypen. A programmable two-qubit quantum processor in silicon. *Nature*, 555(7698):633–637, 2018.

[10] Shama Sharma and Vishwamittar. Brownian motion problem: Random walk and beyond. *Resonance*, 10(8):49–66, 2005.

[11] P H Cootner. *The random character of stock market prices*. M.I.T. Press, 1964.

[12] Andrew M. Childs, Edward Farhi, and Sam Gutmann. An example of the difference between quantum and classical random walks. (2):1–4, 2001.

[13] Andrew M. Childs, Richard Cleve, Enrico Deotto, Edward Farhi, Sam Gutmann, and Daniel A. Spielman. Exponential algorithmic speedup by quantum walk. pages 59–68, 2002.

[14] Yinggan Tang, Xiumei Zhang, Xiaoli Li, and Xinping Guan. Application of a new image segmentation method to detection of defects in castings. *The International Journal of Advanced Manufacturing Technology*, 43(5-6):431–439, 2009.

[15] Jian Li, Xiaolong Li, Bin Yang, and Xingming Sun. Segmentation-based image copy-move forgery detection scheme. *IEEE Transactions on Information Forensics and Security*, 10(3):507–518, 2015.

[16] P. Suetens, E. Bellon, D. Vandermeulen, M. Smet, G. Marchal, J. Nuyts, and L. Mortelmans. Image segmentation: methods and applications in diagnostic radiology and nuclear medicine. *European Journal of Radiology*, 17(1):14–21, 1993.

[17] Zhen Ma, João Manuel, R S Tavares, Renato Natal, and T Mascarenhas. A Review of Algorithms for Medical Image Segmentation and their Applications to the Female Pelvic Cavity A Review of Algorithms for Medical Image Segmentation and their Applications to the Female Pelvic Cavity. *Computer methods of biomechanical and biomedical engineering*, 13(2):235–246, 2010.

[18] Song Yuheng and Yan Hao. Image Segmentation Algorithms Overview. *CoRR*, abs/1707.0, 2017.

[19] Robert M. Haralick and Linda G. Shapiro. Image segmentation techniques. *Computer Vision, Graphics, and Image Processing*, 29(1):100–132, 1985.

[20] Nikhil R. Pal and Sankar K. Pal. A review on image segmentation techniques. *Pattern Recognition*, 26(9):1277–1294, 1993.

[21] Nobuyuki Otsu. A Threshold Selection Method from Gray-Level Histograms. *IEEE Transactions on Systems, Man, and Cybernetics*, 9(1):62–66, 1979.

[22] Nor Mat Isa, Samy Salamah, and Umi Ngah. Adaptive fuzzy moving K-means clustering algorithm for image segmentation. *IEEE Transactions on Consumer Electronics*, 55(4):2145–2153, 2009.

[23] D Ziou and Salvatore Tabbone. Edge detection techniques - an overview. *Pria*, pages 1–41, 1998.

[24] I Sobel. An isotropic 3x3 gradient operator. *Machine Vision for Three-Dimensional Scenes*, (June):376–379, 1990.

[25] D. Marr and E. Hildreth. Theory of edge detection. *Proceedings of the Royal Society of London - Biological Sciences*, 207(1167):187–217, 1980.

[26] Jianbo Shi and Jitendra Malik. Normalized cuts and image segmentation. *IEEE Transactions on Pattern Analysis and Machine Intelligence*, 22(8):888–905, 2000.

[27] Y.Y. Boykov and M.-P. Jolly. Interactive graph cuts for optimal boundary & region segmentation of objects in N-D images. *Proceedings Eighth IEEE International Conference on Computer Vision. ICCV 2001*, 1(July):105–112, 2001.

[28] Eric N. Mortensen and William A. Barrett. Interactive Segmentation with Intelligent Scissors. *Graphical Models and Image Processing*, 60(5):349–384, 1998.

[29] Leo Grady and Eric L. Schwartz. Isoperimetric graph partitioning for image segmentation. *IEEE Transactions on Pattern Analysis and Machine Intelligence*, 28(3):469–475, 2006.

[30] Jonathan Long, Evan Shelhamer, and Trevor Darrell. Fully Convolutional Networks for Semantic Segmentation. 2014.

[31] Vijay Badrinarayanan, Alex Kendall, and Roberto Cipolla. SegNet: A Deep Convolutional Encoder-Decoder Architecture for Image Segmentation. *IEEE Transactions on Pattern Analysis and Machine Intelligence*, 39(12):2481–2495, 2017.

[32] Liang Chieh Chen, George Papandreou, Iasonas Kokkinos, Kevin Murphy, and Alan L. Yuille. DeepLab: Semantic Image Segmentation with Deep Convolutional Nets, Atrous Convolution, and Fully Connected CRFs. *IEEE Transactions on Pattern Analysis and Machine Intelligence*, 40(4):834–848, 2017.

[33] Liang-Chieh Chen, George Papandreou, Florian Schroff, and Hartwig Adam. Rethinking Atrous Convolution for Semantic Image Segmentation. *CoRR*, abs/1706.0, 2017.

[34] Kostas Haris, Serafim N. Efstratiadis, Nicos Maglaveras, and Aggelos K. Katsaggelos. Hybrid image segmentation using watersheds and fast region merging. *IEEE Transactions on Image Processing*, 7(12):1684–1699, 1998.

[35] Nayak Ashwin and Vishwanath Ashvin. Quantum Walk on the Line. Technical report, 2000.

[36] Andris Ambainis. Quantum walks and their algorithmic applications. *International Journal of Quantum Information*, 01(04):507–518, 2004.

[37] Lov K. Grover. A fast quantum mechanical algorithm for database search. In *Proceedings of the twenty-eighth annual ACM symposium on Theory of computing - STOC '96*, pages 212–219, 1996.

[38] Neil Shenvi, Julia Kempe, and K. Birgitta Whaley. Quantum random-walk search algorithm. *Physical Review A - Atomic, Molecular, and Optical Physics*, 67(5):11, 2003.

[39] Andris Ambainis, Julia Kempe, and Alexander Rivosh. Coins Make Quantum Walks Faster. 2004.

[40] Mario Szegedy. Quantum Speed-Up of Markov Chain Based Algorithms. In *Proceedings of the 45th Annual IEEE Symposium on Foundations of Computer Science*, FOCS '04, pages 32–41, Washington, DC, USA, 2004. IEEE Computer Society.

[41] Frederic Magniez, Ashwin Nayak, Jeremie Roland, and Miklos Santha. Search via Quantum Walk. *SIAM Journal on Computing*, 40(1):142, 2011.

[42] Andris Ambainis. Quantum walk algorithm for element distinctness. 0354:1–33, 2003.

[43] Andrew M. Childs and Jason M. Eisenberg. Quantum algorithms for subset finding. *Quantum Information and Computation*, 5(7):593–604, 2005.

[44] Yu-Guang Yang, Qing-Xiang Pan, Si-Jia Sun, and Peng Xu. Novel Image Encryption based on Quantum Walks. *Scientific Reports*, 5(1):7784, 2015.

[45] KARL PEARSON. The Problem of the Random Walk, 1905.

[46] L Lovász. Random walks on graphs: A survey. *Combinatorics Paul Erdos is Eighty*, 2(Volume 2):1–46, 1993.

[47] Min Chen and Supervisor Keith Briggs. Mixing time of random walks on graphs. page 69, 2004.

[48] Y. Aharonov, L. Davidovich, and N. Zagury. Quantum random walks. *Physical Review A*, 48(2):1687–1690, 1993.

[49] Dorit Aharonov, Andris Ambainis, Julia Kempe, and Umesh Vazirani. Quantum Walks On Graphs. *Proceedings of the thirty-third annual ACM symposium on Theory of computing - STOC '01*, pages 50–59, 2000.

[50] Brian C Hall. *Lie Groups, Lie Algebras, and Representations*. 2015.

[51] Yakov M. Shnir. *Magnetic monopoles*, volume 23. 2011.

[52] Navin Khaneja and Steffen Glaser. Cartan Decomposition of SU(2ˆn), Constructive Controllability of Spin systems and Universal Quantum Computing. 2000.

[53] David Martin, Charless Fowlkes, Doron Tal, and Jitendra Malik. A database of human segmented natural images and its application to evaluating segmentation algorithms and measuring ecological statistics. *Proceedings of the IEEE International Conference on Computer Vision*, 2:416–423, 2001.

[54] M. Hebenstreit, D. Alsina, J. I. Latorre, and B. Kraus. Compressed quantum computation using a remote five-qubit quantum computer. *Physical Review A*, 95(5), 2017.

[55] J. S. Otterbach, R. Manenti, N. Alidoust, A. Bestwick, M. Block, B. Bloom, S. Caldwell, N. Didier, E. Schuyler Fried, S. Hong, P. Karalekas, C. B. Osborn, A. Papageorge, E. C. Peterson, G. Prawiroatmodjo, N. Rubin, Colm A. Ryan, D. Scarabelli, M. Scheer, E. A. Sete, P. Sivarajah, Robert S. Smith, A. Staley, N. Tezak, W. J. Zeng, A. Hudson, Blake R. Johnson, M. Reagor, M. P. da Silva, and C. Rigetti. Unsupervised Machine Learning on a Hybrid Quantum Computer. 2017.

[56] Radhakrishnan Balu, Daniel Castillo, and George Siopsis. Physical realization of topological quantum walks on IBM-Q and beyond. 2017.

[57] Yutaka Shikano. From discrete time quantum walk to continuous time quantum walk in limit distribution. *Journal of Computational and Theoretical Nanoscience*, 10(7):1558–1570, 2013.

[58] Viv Kendon. A random walk approach to quantum algorithms. (Shor), 2006.

[59] Fabio Sciarrino. Quantum simulation with integrated photonics.

[60] Andris Ambainis, Eric Bach, Ashwin Nayak, Ashvin Vishwanath, and John Watrous. One-dimensional quantum walks. *Proceedings of the thirty-third annual ACM symposium on Theory of computing*, 3:37–49, 2001.

[61] T Schoning. A probabilistic algorithm for k-SAT and constraint satisfaction problems. In *40th Annual Symposium on Foundations of Computer Science*, pages 410–414, 1999.

[62] Salvador Elías Venegas-Andraca. *Quantum Walks for Computer Scientists*, volume 1. 2008.

[63] Howard C. Berg. *Random walks in biology*. Princeton University Press, 1993.

[64] Todd A. Brun, Hilary A. Carteret, and Andris Ambainis. Quantum to classical transition for random walks. *Physical Review Letters*, 91(13):20, 2003.

[65] Stephen Boyd, Persi Diaconis, Jun Sun, and Lin Xiao. Fastest mixing markov chain on a path. *American Mathematical Monthly*, 113(1):70–74, 2006.

[66] Henrique N.Sá Earp and Jiannis K. Pachos. A constructive algorithm for the Cartan decomposition of SU (2N). *Journal of Mathematical Physics*, 46(8), 2005.

[67] Simona Caraiman and Vasile I. Manta. Image segmentation on a quantum computer. *Quantum Information Processing*, 14(5):1693–1715, 2015.

[68] John Watrous. *The Theory of Quantum Information*. Cambridge University Press, 2018.

[69] Julia Kempe. Quantum random walks: An introductory overview. *Contemporary Physics*, 44(4):307–327, 2003.

[70] Peter W. Shor. Polynomial-Time Algorithms for Prime Factorization and Discrete Logarithms on a Quantum Computer. 41(2):303–332, 1995.

[71] Lawrence Page, Sergey Brin, Rajeev Motwani, and Terry Winograd. The PageRank Citation Ranking: Bringing Order to the Web. *World Wide Web Internet And Web Information Systems*, 54(1999-66):1–17, 1998.

[72] Venkatesan Guruswami. Rapidly Mixing Markov Chains: A Comparison of Techniques (A Survey). 2016.

[73] Naoki Masuda and Norio Konno. Return times of random walk on generalized random graphs. *Physical Review E - Statistical Physics, Plasmas, Fluids, and Related Interdisciplinary Topics*, 69(6):7, 2004.

[74] Yutaka Shikano and Hosho Katsura. Notes on inhomogeneous quantum walks. *AIP Conference Proceedings*, 1363(5):151–154, 2011.

[75] J. K. Asboth. Symmetries, Topological Phases and Bound States in the One-Dimensional Quantum Walk. *Physical Review B*, 86(19):195414, 2012.

[76] Roger A. Horn and Charles R. Johnson. *Matrix analysis*. 2013.

[77] M. Štefaňák, T. Kiss, and I. Jex. Recurrence of biased quantum walks on a line. *New Journal of Physics*, 11, 2009.

[78] Edward Farhi and Sam Gutmann. Quantum computation and decision trees. *Physical Review A*, 58(2):915–928, 1998.

[79] S. E. Venegas-Andraca and J. L. Ball. Processing images in entangled quantum systems. *Quantum Information Processing*, 9(1):1–11, 2010.

[80] Viv Kendon. Quantum walks on general graphs. *International Journal of Quantum Information*, 4(5):791–805, 2003.

[81] Jordi Pont-Tuset. *Image Segmentation Evaluation and Its Application to Object Detection*. PhD thesis, 2014.

[82] Stefanie Barz, Ivan Kassal, Martin Ringbauer, Yannick Ole Lipp, Borivoje Dakic, Alán Aspuru-Guzik, and Philip Walther. Solving systems of linear equations on a quantum computer. pages 1–11, 2013.

[83] Todd Tilma, Mark S. Byrd, and E. C. G. Sudarshan. A Parametrization of Bipartite Systems Based on SU(4) Euler Angles. (4), 2002.

[84] Yutaka Shikano, Tatsuaki Wada, and Junsei Horikawa. Discrete-time quantum walk with feed-forward quantum coin. *Scientific Reports*, 4:4427, 2014.

[85] Mark Kac. Random Walk and the Theory of Brownian Motion. *The American Mathematical Monthly*, 54(7):369, aug 1947.

[86] M. C. Bañuls, C. Navarrete, A. Pérez, Eugenio Roldán, and J. C. Soriano. Quantum walk with a time-dependent coin. *Physical Review A - Atomic, Molecular, and Optical Physics*, 73(6), 2006.

[87] Hai Sheng Li, Zhu Qingxin, Song Lan, Chen Yi Shen, Rigui Zhou, and Jia Mo. Image storage, retrieval, compression and segmentation in a quantum system. *Quantum Information Processing*, 12(6):2269–2290, 2013.

[88] Norio Konno. Continuous-time quantum walks on ultrametric spaces. *International Journal Of Quantum Information*, 4(6):1023–1035, 2006.

[89] Andris Ambainis. Quantum search algorithms. pages 1–12, 2005.

[90] C. M. Chandrashekar, R. Srikanth, and Raymond Laflamme. Optimizing the discrete time quantum walk using a SU(2) coin. *Physical Review A - Atomic, Molecular, and Optical Physics*, 77(3):1–5, 2008.

[91] Salvador Elías Venegas-Andraca. Quantum walks: A comprehensive review. *Quantum Information Processing*, 11(5):1015–1106, 2012.